

Dynamic Graphical Models: Theory, Structure and Counterfactual Forecasting

Luke Vrotsos & Mike West

October 10, 2024

Abstract

Simultaneous graphical dynamic linear models (SGDLMs) provide advances in flexibility, parsimony and scalability of multivariate time series analysis, with proven utility in forecasting. Core theoretical aspects of such models are developed, including new results linking dynamic graphical and latent factor models. Methodological developments extend existing Bayesian sequential analyses for model marginal likelihood evaluation and counterfactual forecasting. The latter, involving new Bayesian computational developments for missing data in SGDLMs, is motivated by causal applications. A detailed example illustrating the models and new methodology concerns global macroeconomic time series with complex, time-varying cross-series relationships and primary interests in potential causal effects.

Keywords: Bayesian forecasting, Causal prediction, Graphical models, Decouple/recouple, Simultaneous graphical dynamic linear models, Sparse dynamic latent factor models.

Affiliations and contact information:

[Luke Vrotsos](#), PhD student in Statistical Science & corresponding author
luke.vrotsos@duke.edu

[Mike West](#), The Arts & Sciences Distinguished Professor Emeritus of Statistics & Decision Sciences
mike.west@duke.edu

Department of Statistical Science, Duke University, Durham, NC 27708-0251, U.S.A.

1 Introduction

Simultaneous graphical dynamic linear models (SGDLMs: [Gruber and West, 2016, 2017](#)) define flexible and scalable multivariate time series structures amenable to efficient Bayesian computations for sequential filtering and forecasting. The models combine parsimonious, customised representations of univariate series with sparse, time-varying representations of cross-series relationships. These advances underlie the adoption of SGDLMs for applications in areas such as financial forecasting and portfolio analysis (e.g. [Griveau-Billion and Calderhead, 2021](#); [Kyakutwika and Bartlett, 2024](#)) with related developments of efficient software (e.g. [Gruber, 2018](#); [Kyakutwika, 2023](#); [Xu, 2024](#)).

For a q -vector time series \mathbf{y}_t , the core representation of a model in the SGDLM class is

$$(\mathbf{I} - \mathbf{\Gamma}_t)\mathbf{y}_t = \boldsymbol{\mu}_t + \boldsymbol{\nu}_t \text{ with } \boldsymbol{\nu}_t \sim \mathbf{N}(\mathbf{0}, \boldsymbol{\Lambda}_t^{-1}) \quad (1)$$

where: (i) the q -vector $\boldsymbol{\mu}_t$ has terms such as trends and regressions on external predictors; (ii) the $q \times q$ matrix $\mathbf{\Gamma}_t$ is sparse and has zero diagonal elements; (iii) $\boldsymbol{\Lambda}_t$ is $q \times q$ diagonal with positive residual volatilities as diagonal elements. These structural models includes time-varying vector-autoregressions and related multivariate volatility models as special cases. Such forms have been widely used in macroeconomics (e.g. [Primiceri, 2005](#); [Bańbura et al., 2010](#); [Koop and Korobilis, 2010, 2013](#); [Nakajima and West, 2013a](#); [Zhao et al., 2016](#); [Lopes et al., 2022](#)) and other areas of signal processing (e.g. [Nakajima and West, 2015, 2017](#)) but with $\mathbf{\Gamma}_t$ strictly triangular. SGDLMs remove that constraint, obviating the issue of dependence on a chosen order of the univariate series in \mathbf{y}_t , and yielding more flexible and parsimonious models. A further advance is in efficient forward simulation and variational Bayes methodology for filtering and forecasting analyses, eliminating the need for intensive and repeat batch MCMC analyses used in most of the prior literature.

The current paper: (i) introduces the modelling framework to a broader research community interested in multivariate time series forecasting in other areas for which these models are suited; (ii) details aspects of the theoretical structure of such models; (b) presents new graphical model theory defined by SGDLMs linked to latent factor structure in multivariate series and systems; and (d) extends the Bayesian methodology for fitting and using SGDLMs in new areas for counterfactual forecasting relevant to casual analysis in time series, with detailed application in that setting. Section 2 discusses aspects of structure with new theory linking graphical and factor models. Section 3 overviews Bayesian filtering and forecasting analyses in SGDLMs, highlighting the relevance of the new theory of Section 2 and adding new developments related to marginal likelihood evaluation for model and hyper-parameter comparisons. Section 4 discusses causal prediction, and develops key extensions of the SGDLM methodology for the setting of partial observations central to counterfactual forecasting relevant in casual analyses. Section 5 develops and explores a detailed example illustrating the new theory and methodology. Section 6 adds summary comments. A detailed Appendix has supporting material on both theory and the examples.

2 Graphical Model Structure and Theory

Discussion of general theory in this section is presented without the time t index, for clarity. For a single observation $\mathbf{y} = (y_1, \dots, y_q)'$, eqn. (1) has the structural form $\mathbf{y} = \boldsymbol{\mu} + \boldsymbol{\Gamma}\mathbf{y} + \boldsymbol{\nu}$ with $V(\boldsymbol{\nu}) = \mathbf{V} = \boldsymbol{\Lambda}^{-1}$. Assume all parameters are known. Given a pattern of zeros in $\boldsymbol{\Gamma}$, each y_i is regressed on only those other y_j for which the i, j element γ_{ij} of $\boldsymbol{\Gamma}$ is non-zero. This is reflected in the directed (but usually *not* acyclic) graph where this set of the y_j are *simultaneous parents* of y_i , denoted by $sp(i) = \{j = 1:q, j \neq i : \gamma_{ij} \neq 0\}$. This y_i is a *child* of each of its parents; the *child set* of any y_j is $ch(j) = \{i = 1:q, i \neq j : \gamma_{ij} \neq 0\}$. Then, $\mathbf{I} - \boldsymbol{\Gamma}$ is non-singular (Appendix B) so that $\mathbf{y} \sim N(\boldsymbol{\alpha}, \boldsymbol{\Omega}^{-1})$ with mean $\boldsymbol{\alpha} = (\mathbf{I} - \boldsymbol{\Gamma})^{-1}\boldsymbol{\mu}$ and precision matrix $\boldsymbol{\Omega} = (\mathbf{I} - \boldsymbol{\Gamma}')\boldsymbol{\Lambda}(\mathbf{I} - \boldsymbol{\Gamma})$.

2.1 Impact of Parental Specification

Impact on Mean. The point prediction α_i of y_i in $\boldsymbol{\alpha} = (\mathbf{I} - \boldsymbol{\Gamma})^{-1}\boldsymbol{\mu}$ will generally have terms involving μ_j for $j \neq i$ as well as μ_i , i.e., “spillover” from some other series. Insights into this are easily appreciated in cases (typical in practice) that $|\boldsymbol{\Gamma}| < 1$ so that $(\mathbf{I} - \boldsymbol{\Gamma})^{-1} = \mathbf{I} + \boldsymbol{\Gamma} + \boldsymbol{\Gamma}^2 + \boldsymbol{\Gamma}^3 + \dots$. Then

$$\alpha_i = \mu_i + \sum_{j \in sp(i)} \gamma_{ij} \mu_j + \sum_{\substack{j \in sp(i) \\ k \in sp(j)}} \{\gamma_{ij} \gamma_{jk}\} \mu_k + \sum_{\substack{j \in sp(i) \\ k \in sp(j) \\ h \in sp(k)}} \{\gamma_{ij} \gamma_{jk} \gamma_{kh}\} \mu_h + \dots$$

This shows the cascade of effects through parental generations. Direct parents have main effects: μ_j contributes to α_i with coefficient γ_{ij} when $j \in sp(i)$. Parents of parents, i.e., grandparents, have second-order effects: μ_k contributes to α_i with a coefficient that sums the products $\gamma_{ij} \gamma_{jk}$ over $j \in sp(i)$ when $k \in sp(j)$. Here series j is a mediating variable between i and k if $k \neq sp(i)$. A grandparent y_k of y_i can also be a parent; then the grandparental term is a second-order interaction relative to the main effect of series k . In typical applications, higher ancestors in the infinite sum have inevitably smaller contributions; successive terms have products of 3, then 4, etc. of the γ_{**} coefficients, which decay to zero at higher generations (since the infinite sum converges).

Impact on Precision. $\boldsymbol{\Omega}$ will typically be sparse, increasingly so with higher sparsity in $\boldsymbol{\Gamma}$. The existence and pattern of off-diagonal zeroes in $\boldsymbol{\Omega}$ relates to the parental structure in the implied, unique undirected graphical model for $p(\mathbf{y})$. A zero off-diagonal element ω_{ij} implies complete conditional independence of y_i, y_j given all other series. We have $\boldsymbol{\Omega} = \mathbf{I} - \boldsymbol{\Gamma}\boldsymbol{\Lambda} - \boldsymbol{\Lambda}\boldsymbol{\Gamma}' + \boldsymbol{\Gamma}'\boldsymbol{\Lambda}\boldsymbol{\Gamma}$. The terms $\boldsymbol{\Gamma}\boldsymbol{\Lambda}$ and $\boldsymbol{\Lambda}\boldsymbol{\Gamma}'$ contribute to a non-zero ω_{ij} if either $i \in sp(j)$ or $j \in sp(i)$, or both. The final term $\boldsymbol{\Gamma}'\boldsymbol{\Lambda}\boldsymbol{\Gamma}$ contributes a non-zero term if y_i, y_j are common parents of any other series y_k , i.e., acts to introduce moralizing edges (marrying any unmarried pairs of parents).

The *simultaneous conditional* p.d.f.s $p_i(y_i | sp(i))$ defined by the model are not, in general, the same as the implied *complete conditionals* $p(y_i | \mathbf{y}_{-i}) \propto p(\mathbf{y})$. See this by inspecting the zero/non-zero patterns off-diagonal in $\boldsymbol{\Omega}$ discussed above. The differences arise either from series $j \notin sp(i)$ with $i \in sp(j)$ (i.e., j is a child of i but not vice versa) or from moralization induced by common parents of a child in the simultaneous system.

2.2 Parental and Child Set Intersections, and Eigenstructure

The set of univariate series y_i for which $ch(i)$ is non-empty can be partitioned into a collection of $k \leq q$ common parental sets $\mathcal{P}_h, h = 1 : k$, such that: (i) each series i belongs to one and only one of the \mathcal{P}_h ; (ii) each series $i \in \mathcal{P}_h$ shares at least one child with at least one of the other series $j \in \mathcal{P}_h$; and (iii) if series $i \in \mathcal{P}_h$ then $ch(i) \cap ch(j) = \emptyset$, the empty, for all series $j \neq \mathcal{P}_h$. Some of the \mathcal{P}_h may include a single series, while those series that are not parental predictors at all are not members of any of the \mathcal{P}_h . Any two series in the same common parental set may not be connected as a parent/child pair themselves. Extend the $ch(\cdot)$ notation to subsets of series with $ch(\mathcal{P}_h)$ being the set of child series of all parental series in \mathcal{P}_h . Write $p_h = \min(|\mathcal{P}_h|, |ch(\mathcal{P}_h)|)$ where $|\cdot|$ denotes the number of series in a subset, and set $p = \sum_{h=1:k} p_h$.

Take the spectral decomposition $\mathbf{\Gamma}'\mathbf{\Gamma} = \mathbf{S}'\mathbf{D}^2\mathbf{S}$. The rows of \mathbf{S} are the eigenvectors of $\mathbf{\Gamma}'\mathbf{\Gamma}$; the eigenvalues defining the diagonal matrix \mathbf{D}^2 are the squares of the singular values of $\mathbf{\Gamma}$, some of which may be zero. The i,j off-diagonal element of $\mathbf{\Gamma}'\mathbf{\Gamma}$ is non-zero when variables i,j are common parents of one or more children, i.e., if $ch(i) \cap ch(j) \neq \emptyset$. With no loss of generality, order variables so that the first p_1 are those in \mathcal{P}_1 , followed by those in \mathcal{P}_2 , and so forth, continuing to finally include any remaining series that have no child series in arbitrary order. With this ordering, $\mathbf{\Gamma}'\mathbf{\Gamma} = \text{block diag}(\mathbf{\Phi}_1, \dots, \mathbf{\Phi}_k, \mathbf{0})$ with symmetric $p_h \times p_h$ matrices $\mathbf{\Phi}_h$ for $h = 1 : k$, followed by a $(q - p) \times (q - p)$ $\mathbf{0}$ matrix. Each $\mathbf{\Phi}_h$ may or may not have some off-diagonal zeros; the non-zeros correspond to children shared by two parents in \mathcal{P}_h .

The rows of \mathbf{S} are sparse, each having non-zero values in elements corresponding to only one of the sets \mathcal{P}_h and with values coming from the eigenvectors of the implied $\mathbf{\Phi}_h$ (see, for example, the theory in [Simovici and Djeraba, 2014](#)). When each of the $\mathbf{\Phi}_h$ has full rank p_h , then $p = \text{rank}(\mathbf{\Gamma})$. Call this the *parental full-rank case*; otherwise, the model represents a *parental reduced-rank case* and $p < \text{rank}(\mathbf{\Gamma})$. In practice and in the extension to time series below, reduced rank cases are rare.

2.3 Sparse Factor Structure

The singular value decomposition (SVD) is $\mathbf{\Gamma} = \mathbf{LDS}$ where, with dimension $p \leq q$ equal to the number of non-zero singular values, the $q \times p$ *factor loadings* matrix \mathbf{L} has orthonormal columns, and the $p \times q$ (orthonormal rows) *factor scores* matrix \mathbf{S} and $\mathbf{D} = \text{diag}(d_1, \dots, d_p)'$ has the non-zero singular values of $\mathbf{\Gamma}$. Both \mathbf{S} and \mathbf{D} underlie the eigenstructure of $\mathbf{\Gamma}'\mathbf{\Gamma}$ discussed above. When $\mathbf{\Gamma}$ is sparse, both \mathbf{L} and \mathbf{S} will generally be sparse.

The model $\mathbf{y} = \boldsymbol{\mu} + \mathbf{\Gamma}\mathbf{y} + \boldsymbol{\nu}$ then maps to $\mathbf{y} = \boldsymbol{\mu} + \mathbf{L}\boldsymbol{\eta} + \boldsymbol{\nu}$ with $\boldsymbol{\eta} = (\eta_1, \dots, \eta_p)'$ = \mathbf{DSy} . This is the form of a mean-adjusted factor model with p -dimensional *factor* vector $\boldsymbol{\eta}$ based on the factor loadings matrix \mathbf{L} and the factor scores matrix \mathbf{S} . Each factor η_j is a “linear scalar component” defined by a subset of the variables. Inherently, the implied factors are dependent; $\mathbf{V}(\boldsymbol{\eta}) = \mathbf{DS}\boldsymbol{\Omega}^{-1}\mathbf{S}'\mathbf{D}$ may have important cross-factor correlations. This contrasts with traditional factor models that impose orthogonal factors for mathematical identification reasons that are moot here. The factors are also correlated with the residuals $\boldsymbol{\nu}$. Specifically, $\mathbf{C}(\boldsymbol{\eta}, \boldsymbol{\nu}) = \mathbf{DS}\mathbf{A}\mathbf{V}$ where $\mathbf{A} = (\mathbf{I} - \mathbf{\Gamma})^{-1}$ and \mathbf{V} is the diagonal matrix $\mathbf{V} = \boldsymbol{\Lambda}^{-1}$. While $\mathbf{C}(\boldsymbol{\eta}, \boldsymbol{\nu})$ will typically be very sparse, it may sometimes indicate non-negligible correlations.

The theory in Section 2.2 now shows that number of factors is $p = \sum_{h=1:k} p_h = \text{rank}(\mathbf{\Gamma})$ in the (typical) parental full-rank case. Then, for each $h = 1 : k$ there are p_h rows of \mathbf{S} with non-zero weightings only on the elements of \mathcal{P}_h . The corresponding p_h columns of \mathbf{L} have non-zero entries only for the variables in $ch(\mathcal{P}_h)$. In a parental reduced-rank case, the number of factors is reduced by the sum of the rank deficiencies of the $\mathbf{\Phi}_h$; rows of \mathbf{S} and columns of \mathbf{L} again define factors based on only one of the \mathcal{P}_h , but for any h with $\mathbf{\Phi}_h$ rank deficient, two or more of the implied factors are co-linear. In practice, the full-rank case is the norm; Fang et al. (2024, Theorem 2) shows how to determine whether the graphical structure implies a reduced-rank case.

3 Structure and Analysis of SGDLMs

3.1 SGDLM Specification: Reprise

With $\mathbf{y}_t = (y_{1t}, \dots, y_{qt})'$, each univariate series in the SGDLM of eqn. (1) follows a dynamic linear model (DLM)

$$y_{jt} = \mathbf{F}'_{jt} \boldsymbol{\theta}_{jt} + \nu_{jt}, \quad \nu_{jt} \sim N(0, 1/\lambda_{jt}), \quad \text{and} \quad \boldsymbol{\theta}_{jt} = \mathbf{G}_{jt} \boldsymbol{\theta}_{j,t-1} + \boldsymbol{\omega}_{jt} \quad (2)$$

where the observation noise terms ν_{jt} and evolution innovations $\boldsymbol{\omega}_{jt}$ are zero mean, mutually independent, and independent across series j over time t . This is a traditional model with regression vector $\mathbf{F}_{jt} = (\mathbf{x}_{jt}, \mathbf{y}_{sp(j),t})'$ where subvector \mathbf{x}_{jt} involves predictors (constants, exogenous variables, lagged y_* values, etc.) specific to model j , while $\mathbf{y}_{sp(j),t}$ is a subvector of \mathbf{y}_t with indices in the simultaneous parental set $sp(j)$ that induce cross-series, time-varying conditional dependencies. The Markov-evolving state vector has partitioned form $\boldsymbol{\theta}_{jt} = (\boldsymbol{\phi}_{jt}, \boldsymbol{\gamma}_{jt})'$ conformable with that of \mathbf{F}_{jt} . Thus $\mathbf{F}'_{jt} \boldsymbol{\theta}_{jt} = \mu_{jt} + \mathbf{y}'_{sp(j),t} \boldsymbol{\gamma}_{jt}$ where $\mu_{jt} = \mathbf{x}'_{jt} \boldsymbol{\phi}_{jt}$ is element j of $\boldsymbol{\mu}_t$ in eqn. (1). The (j, h) element of the $q \times q$ matrix $\mathbf{\Gamma}_t$ has the relevant element from $\boldsymbol{\gamma}_{jt}$ for each $h \in sp(j)$, being zero otherwise. Further, $\boldsymbol{\nu}_t = (\nu_{1t}, \dots, \nu_{qt})'$ with precision matrix $\mathbf{\Lambda}_t = \text{diag}(\lambda_{1t}, \dots, \lambda_{qt})$. The rest of the model structure is from standard DLM methodology: the state evolution matrix \mathbf{G}_{jt} is known at time t , the λ_{jt} evolve according to standard beta-gamma Markov processes, and $V(\boldsymbol{\omega}_{jt})$ is defined by discount factors (e.g. Gruber and West, 2016; Prado et al., 2021, chap. 4).

From Section 1, the implied distribution for \mathbf{y}_t is $\mathbf{y}_t \sim N(\boldsymbol{\alpha}_t, \mathbf{\Omega}_t^{-1})$ with $\boldsymbol{\alpha}_t = (\mathbf{I} - \mathbf{\Gamma}_t)^{-1} \boldsymbol{\mu}_t$ and precision matrix $\mathbf{\Omega}_t = (\mathbf{I} - \mathbf{\Gamma}_t)' \mathbf{\Lambda}_t (\mathbf{I} - \mathbf{\Gamma}_t)$. Different external predictors \mathbf{x}_{jt} over j allow customisation of individual models, while small simultaneous parental sets $sp(j)$ induce sparse $\mathbf{\Gamma}_t$ and parsimonious dynamic graphical models via the implied sparsity of $\mathbf{\Omega}_t$.

3.2 Sparse Dynamic Factor Structure

The theory of Section 2.3 yields the implied, dynamic sparse factor model form $\mathbf{y}_t = \boldsymbol{\alpha}_t + \mathbf{L}_t \boldsymbol{\eta}_t + \boldsymbol{\nu}_t$ where, based on the SVD $\mathbf{\Gamma}_t = \mathbf{L}_t \mathbf{D}_t \mathbf{S}_t$, the factor vector is $\boldsymbol{\eta}_t = \mathbf{D}_t \mathbf{S}_t \mathbf{y}_t$. The theory of Section 2.3 applies directly here to inform on the number of factors p . In this time series setting, there are evident connections with “linear scalar components” that aim to “reveal possibly hidden simplifying structures of the process” (e.g. Tiao and Tsay, 1989). The broader connections are with the rich

literature on sparse and dynamic latent factor modelling (e.g. Lopes and Carvalho, 2007; Nakajima and West, 2013b; Kaufmann and Schumacher, 2019; Lavine et al., 2022; Bolfarine et al., 2024, and references therein) In the new perspective here, however, the factor structure is derivative of the general graphical modelling approach, and the sparsity patterns in the (time-varying) $q \times p$ loadings matrix \mathbf{L}_t and $p \times q$ scores matrix \mathbf{S}_t are determined wholly by the choice of parental sets.

Again from Section 2.3, the variance matrix $V(\boldsymbol{\eta}_t) = \mathbf{D}_t \mathbf{S}_t \boldsymbol{\Omega}_t^{-1} \mathbf{S}_t' \mathbf{D}_t$ may have strong cross-factor dependencies. It is important to note that other approaches to dynamic *dependent* factor modelling have shown improvements in model fit and forecasting accuracy– and to a degree interpretations– with models that allow cross-factor correlations; in some such cases, the data analysis infers strong factor-factor dependencies (e.g. Nakajima and West, 2013b; Zhou et al., 2014).

3.3 Filtering and Forecasting in SGDLMs

The sequential analysis of SGDLMs integrates standard theory and methodology of univariate DLM analysis into the multivariate simultaneous system with a decouple/recouple strategy (West, 2020). Analysis is sequential over time, with time $t - 1$ to t forecast-update-evolution steps that are recursively applied as time t evolves. The detailed analytic framework (Gruber and West, 2016, 2017) is summarised in relevant aspects in Appendix A. The analysis combines decoupled, conditionally conjugate priors and posteriors for states and volatilities $\{\boldsymbol{\theta}_{jt}, \lambda_{jt}\}$ in each time period, with analytic updating in the corresponding univariate DLMs that are then recoupled to define full inferences on the set of dynamic parameters $\boldsymbol{\Theta}_t = [\boldsymbol{\theta}_{1t}, \dots, \boldsymbol{\theta}_{qt}]$ and $\boldsymbol{\Lambda}_t = \text{diag}(\lambda_{1t}, \dots, \lambda_{qt})$ in the multivariate system of eqn. (2). Full inference and multi-step ahead forecasting at each time point exploits simple importance sampling (IS) for prior-posterior updates and direct simulation for forecasting. Moving posterior distributions through the state and volatility evolutions of the model at each time (i) decouples the series into their univariate models, and (ii) exploits accurate Variational Bayes (VB) steps that link importance sample posterior representations to conditionally conjugate forms that enable analytic updating. See Appendix A for summary details.

3.4 Marginal Likelihoods in SGDLMs

One contribution of the current paper is to define Monte Carlo evaluation of model marginal likelihoods– for model and hyper-parameter comparison– in SGDLMs. These require evaluations of the 1–step predictive p.d.f.s $p(\mathbf{y}_t | \mathcal{D}_{t-1}) = E[p(\mathbf{y}_t | \boldsymbol{\Theta}_t, \boldsymbol{\Lambda}_t, \mathcal{D}_{t-1})]$ where the expectation is over the time t prior $p(\boldsymbol{\Theta}_t, \boldsymbol{\Lambda}_t | \mathcal{D}_{t-1})$. The marginal likelihood from data over a series of times is the product of the per time t values.

A direct approximation of $p(\mathbf{y}_t | \mathcal{D}_{t-1})$ is a sample average of $p(\mathbf{y}_t | \boldsymbol{\Theta}_t, \boldsymbol{\Lambda}_t, \mathcal{D}_{t-1})$ over draws from the prior $p(\boldsymbol{\Theta}_t, \boldsymbol{\Lambda}_t | \mathcal{D}_{t-1})$. However, a provably more accurate Monte Carlo approximation is based on sampling the *posterior* rather than the prior. The relevant supporting theory and details in Appendix C are summarised here.

With time t prior of the product conjugate form in eqn. (4) of Appendix A, we have

$$p(\mathbf{y}_t|\mathcal{D}_{t-1}) = \int |\mathbf{I} - \mathbf{\Gamma}_t|_+ \prod_{j=1}^q p_j(y_{jt}|\mathbf{y}_{sp(j)t}, \boldsymbol{\theta}_{jt}, \lambda_{jt}, \mathcal{D}_{t-1}) p_j(\boldsymbol{\theta}_{jt}, \lambda_{jt}|\mathcal{D}_{t-1}) d\boldsymbol{\Theta}_t d\boldsymbol{\Lambda}_t.$$

This reduces to $p(\mathbf{y}_t|\mathcal{D}_{t-1}) = g_t(\mathbf{y}_t) \prod_{j=1}^q p_j(y_{jt}|\mathbf{y}_{sp(j)t}, \mathcal{D}_{t-1})$ where

$$g_t(\mathbf{y}_t) = \int |\mathbf{I} - \mathbf{\Gamma}_t|_+ \prod_{j=1}^q p_j(\boldsymbol{\gamma}_{jt}|y_{jt}, \mathbf{y}_{sp(j)t}, \mathcal{D}_{t-1}) d\mathbf{\Gamma}_t$$

in which: (i) $p_j(y_{jt}|\mathbf{y}_{sp(j)t}, \mathcal{D}_{t-1})$ is the prior predictive T p.d.f in series j , and (ii) the p.d.f. $p_j(\boldsymbol{\gamma}_{jt}|y_{jt}, \mathbf{y}_{sp(j)t}, \mathcal{D}_{t-1})$ is that of the marginal *posterior* T distribution for the subvector $\boldsymbol{\gamma}_{jt}$ in the model for series j . This explicitly shows how the computational challenge arises only through the simultaneous parental parameters $\mathbf{\Gamma}_t$ with the implied need to approximate $g_t(\mathbf{y}_t)$.

Monte Carlo integration approximates $g_t(\mathbf{y}_t)$ with a sample average of $|\mathbf{I} - \mathbf{\Gamma}_t|_+$ over independent draws of the $\boldsymbol{\gamma}_{jt}$ from their marginal T posteriors. Compared to sampling from the prior, this yields an approximation of $p(\mathbf{y}_t|\mathcal{D}_{t-1})$ with lower Monte Carlo variance due to conditioning on \mathbf{y}_t values and the exploitation of partial analytic terms. Appendix C provides the underlying theory.

4 Counterfactual Analysis for Causal Forecasting

4.1 Background and Setting

Causal inference and forecasting in time series data is an area of increasing research interest in recent years, with a main focus on counterfactual forecasting. The idea of using chosen or constructed “synthetic” control series to condition counterfactual forecasts of putative “treated” or “experimental” series (from [Abadie and Gardeazabal, 2003](#)) is increasingly widespread in economics and other social sciences. Bayesian versions were introduced by [Brodersen et al. \(2015\)](#) for a univariate outcome series, with later work addressing steps into multivariate time series (e.g. [Menchetti and Bojinov, 2022](#); [Antonelli and Beck, 2023](#)).

The canonical setting is that the q series are observed over time prior to an identified event– or intervention– time T . At this time, a subset of the series is regarded as potentially affected, with the rest assumed to be unaffected. The setting will often be observational though we follow prior literature in using “experimental” and “control” for the two sets of series. Reorder the series so that $\mathbf{y}'_t = (\mathbf{y}'_{ct}, \mathbf{y}'_{et})$ with q_c –vector \mathbf{y}_{ct} of controls and q_e –vector \mathbf{y}_{et} of experimental series for $q_c + q_e = q$. The same terminology applies for $t < T$. The counterfactual forecasting focus is to predict $(\mathbf{y}_{et}|\mathbf{y}_{ct})$ for $t > T$ and then assess how such predictions depart from the post– T development of \mathbf{y}_{ct} . over that period. Then, the literature is embracing the more global goal of using all control series together, rather than constructing some inspired summaries of them as synthetic controls ([Tierney et al., 2024](#); [Li et al., 2024](#)). This is our perspective here. Linked to these core goals, a key challenge in the multivariate context is the flexibility of modelling dependencies among series; traditional multivariate models are less flexible and overly constraining, especially for larger series

dimension q . It is especially critical in causal studies to enable sensitive characterisation of pre-intervention dependencies between experimental and control series; counterfactual forecasting is wholly based on that. We also emphasise routine sequential analysis in which the post-intervention inferences monitor potential causal changes, so multivariate time series models that enable sequential analysis are of interest. This is particularly important in terms of learning about cross-series relationships that may change in time. Further, the ability to define a parallel post-intervention analysis that explicitly admits the potential for changes—providing an alternative to the counterfactual hypothesis in the context of evolving, sequential learning from post-intervention data, is a key theme. This relates to a number of interests, including the question of whether some of the putative control series do in fact exhibit post-intervention changes potentially related to the intervention, i.e., so-called interference effects.

4.2 Counterfactual and Outcome Adaptive SGDLMS

Counterfactual Model (CFM). The SGDLMS framework provides opportunity to address the several above goals. Given a pre-intervention SGDLMS fitted over $t = 1 : T$, counterfactual analysis begins under the assumption of no intervention effects. Write \mathbf{y}_{e_0t} for the purely hypothetical counterfactual outcomes for $t \geq T$, the series that would have occurred under this assumption. Pre-intervention, \mathbf{y}_{ct} and $\mathbf{y}_{e_0t} = \mathbf{y}_{et}$ are observed; post-intervention counterfactual analysis assumes only \mathbf{y}_{ct} is observed and \mathbf{y}_{e_0t} is “missing data”. Predictions of \mathbf{y}_{e_0t} are made and successively revised over the post-intervention period to compare with the actual outcomes; denote the latter by \mathbf{y}_{e_1t} . A main contribution of this paper is to extend the technical and computational methodology of SGDLMS analysis to admit such missing data. The existing forward filtering analysis using IS and VB needs to be extended to do this, the former to now include simulation of unobserved potential outcomes \mathbf{y}_{e_0t} post-intervention. This aims to yield full uncertainty quantification for inference on potential causal effects. Refer to the SGDLMS in this setting as the *counterfactual model* (CFM).

Outcome Adaptive Model (OAM). An important methodological development, defined in [Li et al. \(2024\)](#) using other models, is to also consider a separate *outcome adaptive model* (OAM) to be run independently of, and in parallel to, the CFM. The OAM is the same SGDLMS and its analysis involves full observations on $\mathbf{y}_{ct}, \mathbf{y}_{e_1t}$ with one modification at time $T - 1$. At that point only, the univariate DLMS for each of the *experimental series only* are adjusted to allow for potentially higher levels of change in states and volatilities. After updating at time T , the model reverts to precisely as pre-intervention. The mechanism is to simply reduce the state and volatility discount factors at $T - 1$ then revert to their normal, higher values at time T . This is a standard method of responding to the possibility of a causal impact on the e_1 series, allowing the OAM to adapt to, and infer, resulting changes on the explicit assumption that “something may have happened” (e.g. [West and Harrison, 1986, 1997](#), chap. 11). Causal prediction based on comparing inferences from the OAM with those from the CFM provides a formal statistical assessment of the effects. As a side-benefit, exploring post-intervention predictions for each of the designated control series can prove useful in assessing potential interference effects, i.e., to what extent one or more controls may show inheritance of any changes seen in the e_1 series.

4.3 Filtering Updates in CFM

The missingness of \mathbf{y}_{e_0t} complicates post-intervention inference on SGDLM parameters. Conjugate normal-gamma updates for the univariate models cannot be performed if experimental series are either parents or children of other series. In this case, the standard SGDLM filtering analysis breaks down. However, the structure of the model leads to an immediate extension to incorporate the missing data \mathbf{y}_{e_0t} , together with the parameters Θ_t, Λ_t , in a novel Monte Carlo filtering strategy.

The target filtered posterior for $\Theta_t, \Lambda_t, \mathbf{y}_{e_0t}$ at time t has the compositional form

$$p(\Theta_t, \Lambda_t | \mathbf{y}_{ct}, \mathbf{y}_{e_0t}, \mathcal{D}_{t-1}) p(\mathbf{y}_{e_0t} | \mathbf{y}_{ct}, \mathcal{D}_{t-1}).$$

The first term is the standard SGDLM posterior for states and volatilities assuming \mathbf{y}_{e_0t} known. The second term, the marginal posterior for the missing data, is not available analytically but can be accurately approximated as follows. Given the time $t - 1$ prior Monte Carlo sample of states and volatilities, Θ_t^r, Λ_t^r , ($r = 1:R$), the joint time $t - 1$ p.d.f. of $\mathbf{y}_{ct}, \mathbf{y}_{e_0t}$ has direct Monte Carlo approximation given by

$$p(\mathbf{y}_{ct}, \mathbf{y}_{e_0t} | \mathcal{D}_{t-1}) = R^{-1} \sum_{r=1:R} p(\mathbf{y}_{ct}, \mathbf{y}_{e_0t} | \Theta_t^r, \Lambda_t^r, \mathcal{D}_{t-1})$$

where each term is a multivariate normal p.d.f. from the SGDLM. The implied conditional for the missing data \mathbf{y}_{e_0t} given the observed \mathbf{y}_{ct} is then

$$p(\mathbf{y}_{e_0t} | \mathbf{y}_{ct}, \mathcal{D}_{t-1}) = \sum_{r=1:R} \pi_{rt}(\mathbf{y}_{ct}) p(\mathbf{y}_{e_0t} | \mathbf{y}_{ct}, \Theta_t^r, \Lambda_t^r, \mathcal{D}_{t-1}) \quad (3)$$

where the component p.d.f.s are the implied conditional normals for \mathbf{y}_{e_0t} , and the mixture weights $\pi_{rt}(\mathbf{y}_{ct}) \propto p(\mathbf{y}_{ct} | \Theta_t^r, \Lambda_t^r, \mathcal{D}_{t-1})$ simply involve evaluations of the corresponding marginal normal p.d.f.s at \mathbf{y}_{ct} . The strategy is then to generate a sample of \mathbf{y}_{e_0t} from the above mixture of normals, and on each sampled value generate $\Theta_t, \Lambda_t | \mathbf{y}_{ct}, \mathbf{y}_{e_0t}, \mathcal{D}_{t-1}$ with the usual SGDLM importance sampling weights proportional to $|\mathbf{I} - \Gamma_t|_+$. The resulting IS weights will reflect additional variation due to uncertainty about \mathbf{y}_{e_0t} ; this is implicit as each parameter sample relies on its corresponding sampled value of the missing data.

The computational details simply involve multivariate normal density evaluations and multinomial sampling. Technical details related to computational efficiencies, as well as relevant theoretical developments, are given in Appendix D. The MC sample size R can be increased with limited computational demands, and this may be important in improving the resulting IS performance.

5 Application

5.1 Setting and Background

The setting and data concern annual per capita GDP (1960–2003) in a selection of $q = 16$ OECD countries, taken from [Abadie et al. \(2015\)](#). The countries with standard 3–character codes (ordered solely for aesthetics in graphical analysis summaries) are:

Austria (AUT), United States of America (USA), Netherlands (NLD), Portugal (PRT), Belgium (BEL), Norway (NOR), Australia (AUS), France (FRA), Germany (DEU), Italy (ITA), Switzerland (CHE), Denmark (DNK), New Zealand (NZD), United Kingdom (GBR), Spain (ESP) and Japan (JPN).

A key interest here is assessing the impact of 1990 German reunification on German GDP and other countries. This data set has been used to exemplify other causal methodological developments (e.g. [Klößner et al., 2018](#); [Pang et al., 2022](#)). In contrast to these prior analyses, which analyze GDP directly, we model the statistically natural annual log returns $y_{jt} = \log(\text{GDP}_{jt}/\text{GDP}_{j,t-1})$ for country j in year t ; see Figure 1. Contextual predictions then simply transform to the GDP scale. Most importantly, we define a different set of control countries than other analyses. Recognizing the potential for effects of German reunification on economic growth in other countries— especially those in Europe— we designate only Australia and New Zealand as control series. The remaining 14 countries are designated as experimental series along with Germany. In addition to contextual relevance, this moves well beyond prior models in terms of larger numbers of experimental series.

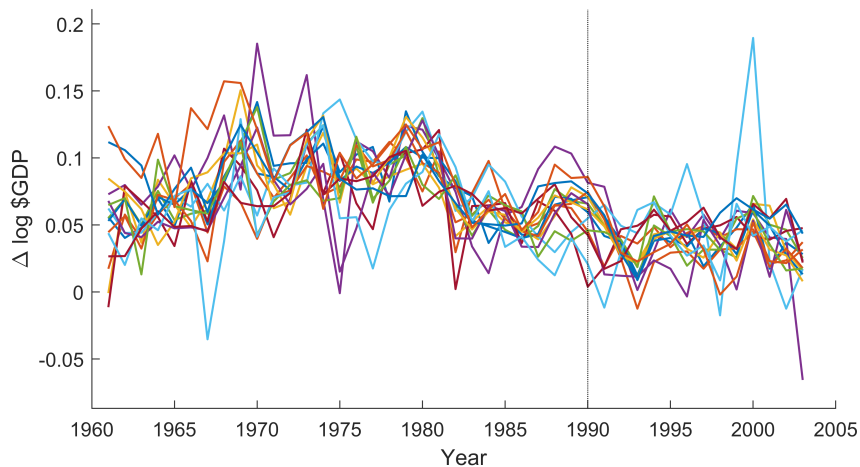


Figure 1: GDP example: Changes in annual log GDP of $q = 16$ countries. The thick line is DEU.

5.2 SGDLM Specification

Model Form. The univariate DLM for each of the $j = 1 : 16$ series has a 3–vector \mathbf{x}_{jt} with first element equal to 1, followed by the lag–1 outcomes of the Australia and New Zealand series. This de-

finds a time-varying, sparse vector autoregressive form for μ_t to (partly) predict short-term changes based on the lagged control series, with local intercepts that can capture otherwise unexplained trends over time. Each series then has either one or two simultaneous parents, displayed in Figure 2. This simultaneous parental graph is selected as an example to underlie the methodological developments of this paper; it is based on simple exploratory analysis of the pre-reunification data alone, noted in Appendix E.1. The implied (conditional independence) graph defining the sparsity pattern in Ω is shown there with additional discussion. We comment further on the broader questions of parental set selection—beyond the scope of the current paper—in Section 6.

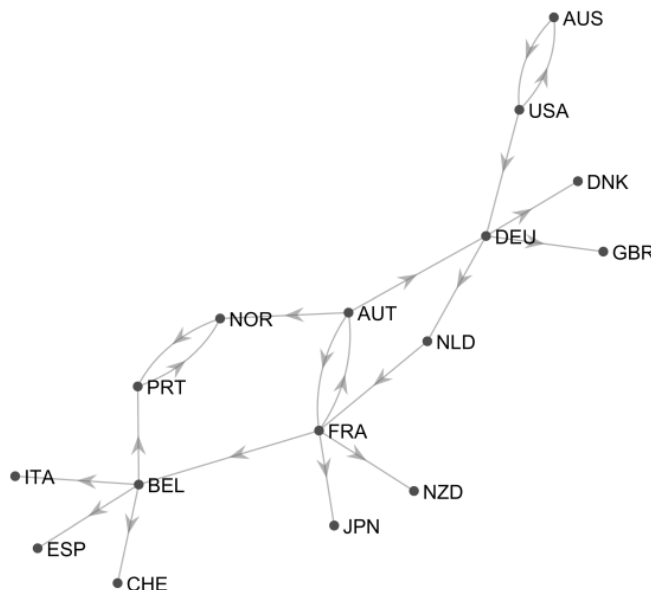


Figure 2: GDP example: Simultaneous parental graph with the $q = 16$ countries as nodes. Directed edges point from parental to child nodes.

Priors and Discount Factors. Time notation replaces $t = 1, 2, \dots$ with years $t = 1960, 1961, \dots$ for contextual clarity. For $j \in 1 : q$, the priors at time $t = 1961$ have $\mathbf{m}_{j,1961}^* = (0.05, 0, \dots, 0)$, $\mathbf{M}_{j,1961}^* = \text{diag}(0.0025, 0.1, \dots, 0.1)$, $n_{j,1961}^* = 4$, and $s_{j,1961}^* = 0.0004$. The prior mean for the intercept of the series is 0.05, representing approximately 5% GDP growth, and the prior mean for all other coefficients is 0. Discount factors are $\delta = 0.95$ for state parameters and $\beta = 0.95$ for volatilities, choices based on evaluating cumulative one-step marginal likelihoods during the pre-intervention period across a grid of plausible values; this uses the new methodology of Section 3.4, and further details are given in Appendix E.3. Finally, the OAM analysis is based on taking $\delta = 0.50$ at (and only at) $t = 1991$ in order that the model be more adaptive to immediate post-intervention data; the OAM analysis reverts to using $\delta = 0.95$ again from $t = 1992$ onwards.

Monte Carlo Analysis. SGDLM analysis is based on $R = 10,000$ Monte Carlo samples for the importance sampling steps each time period. Monitored values of effective sample sizes exceed 90% for all years, indicating a highly efficient Monte Carlo analysis (c.f. Gruber and West, 2016, 2017) over the years. This is true pre- and post-intervention at $t = T = 1990$, after which the

analysis includes the new extensions that add the unobserved counterfactual outcomes on all of the 14 series designated as experimental over the following years. The direct simulation of posteriors for the counterfactual outcomes using the mixture methodology of Section 4.3 is also based on $R = 10,000$ samples each year. Analysis summaries below are based on Monte Carlo samples of filtered posteriors over time for state vectors and volatilities, and corresponding predictive distributions for future outcomes including the counterfactuals of causal interest.

5.3 Counterfactual Forecasting

Figure 3 shows filtered posteriors for y_{e_0t} at each year t in the standard SGDLM (pre-1990) and the CFM (post-1990), with actual outcomes superimposed, for Germany, Austria and the United Kingdom. Figure 4 transforms these to the original GDP scale. Post-1990, all three countries have GDP growth below what would be expected under the counterfactual, but the departure from this trend is most striking in Germany, especially in 1992-1994. Based on the observed values of the controls, we would expect a slight increase in German GDP growth in the first two years after reunification; instead, we observe a sharp drop-off. Uncertainty in the counterfactual forecasts naturally increases over time post-1990.

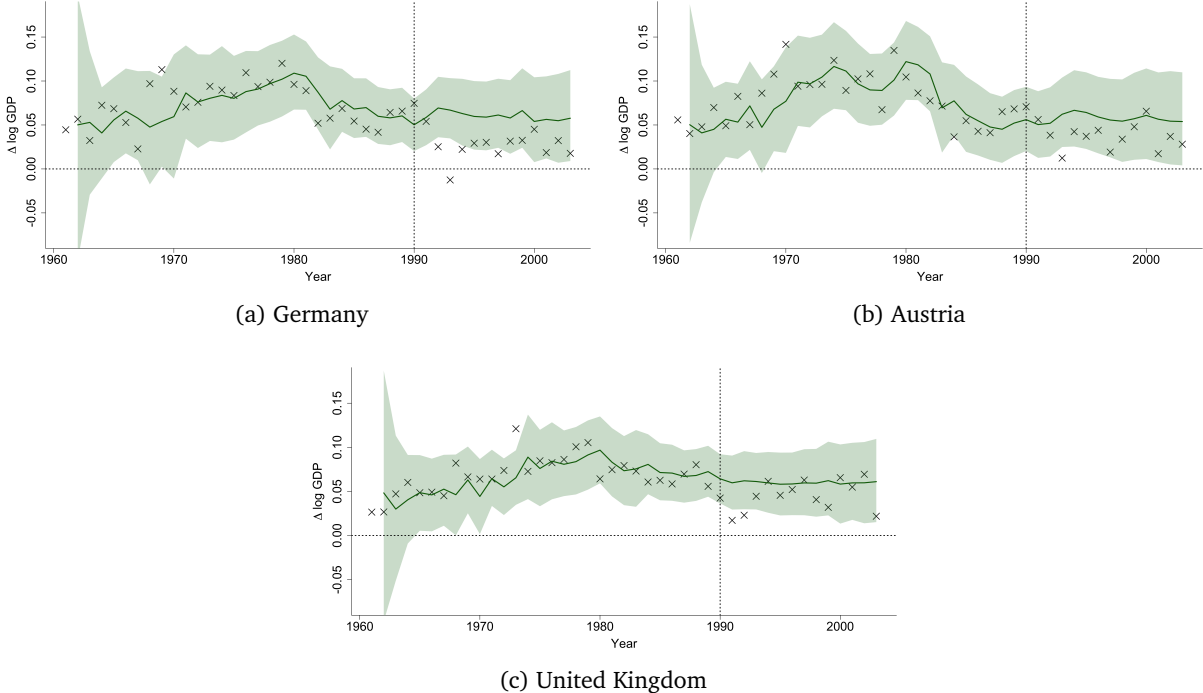


Figure 3: GDP example: Trajectories of inferences on elements of y_{e_0t} for 3 countries, in terms of time t filtered posterior medians (full line) and equal-tails 90% intervals (shading), with outcomes (crosses) superimposed. Prior to $T = 1990$ these represent model “fit”; after intervention they are pure counterfactual predictions.

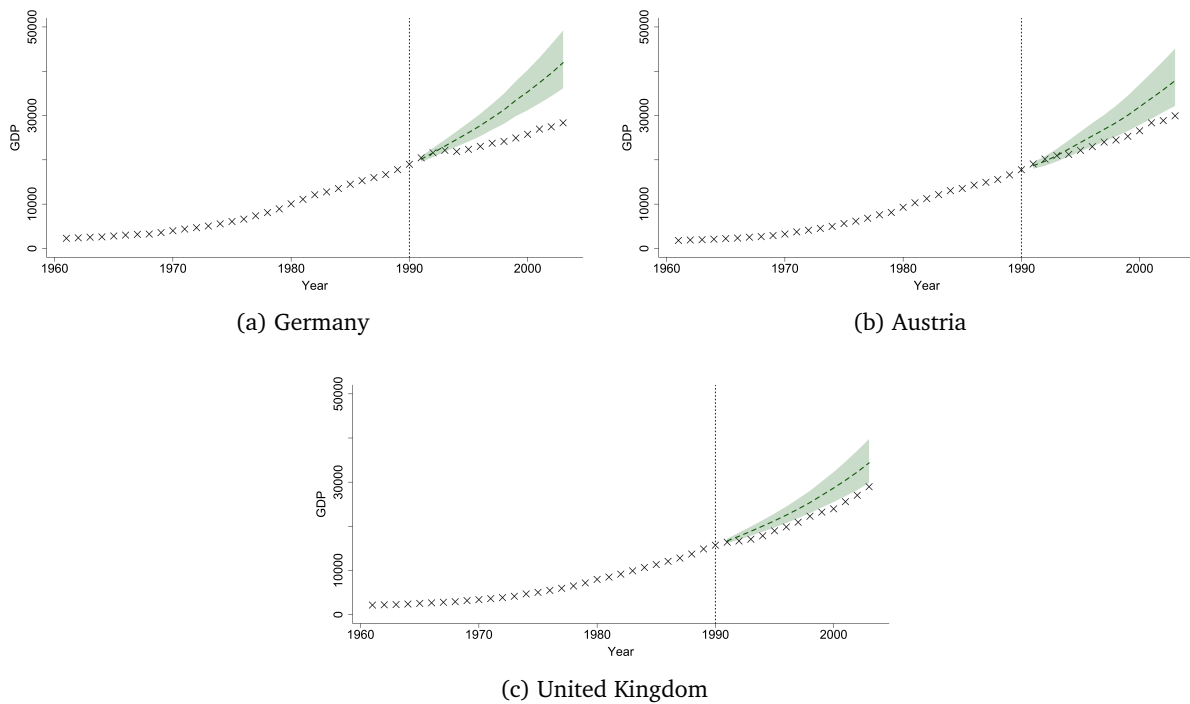


Figure 4: GDP example: Trajectories as in Figure 3 transformed to the actual GDP scale.

Figure 5 shows inferred trajectories of the difference in model means $F'_{jt}\theta_{jt}$ between the CFM and OAM. This highlights departure of beliefs about the expected level of GDP growth accounting for the inevitable year-to-year stochastic variation. The trajectories for all three countries favour negative values, most substantially for Germany immediately post-intervention. For GBR, the initially negative effect diminishes later in the post-intervention period. Along with several other European countries not pictured, the effect for Austria favours negative values for most of the post-intervention period, although smaller in magnitude than that of Germany and with credible intervals generally including 0. These findings indicate a possible spillover effect of German reunification on series other countries.

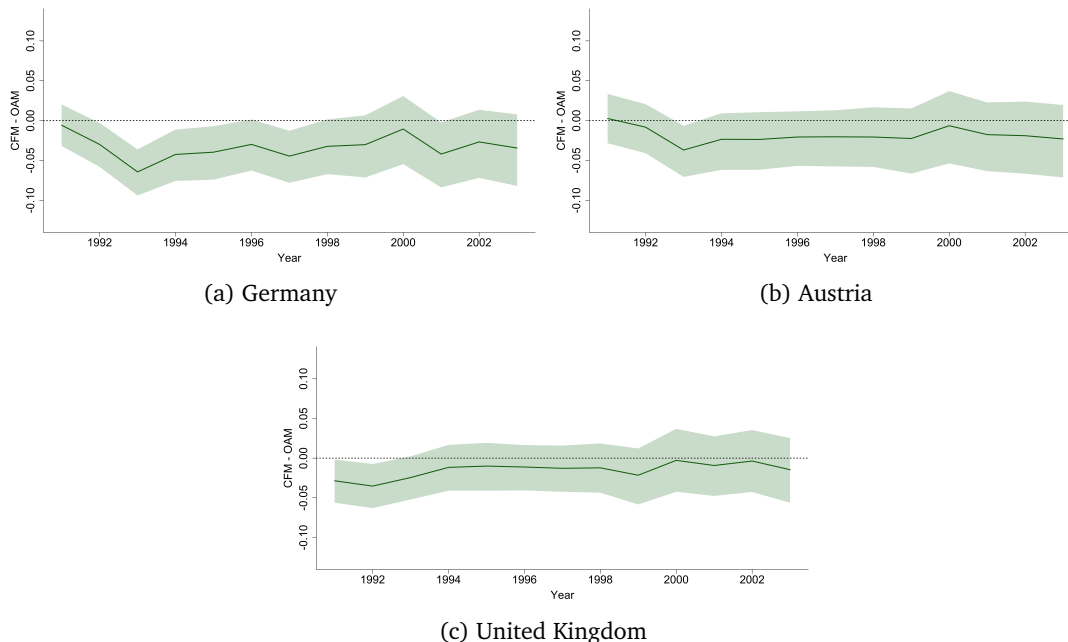


Figure 5: GDP example: Difference in filtered mean forecasts between the CFM and OAM.

5.4 Parental Regression Coefficients

Time trajectories of posteriors for the γ_{ijt} inform on changing cross-series relationships; this is of general interest while being more specifically relevant post-intervention. Figure 6 displays this for coefficients of Germany on Austria and USA in both the CFM and OAM. These show an immediate post-intervention effect with the simultaneous predictive role of Austria increasing and that of the USA decreasing. The OAM adapts and highlights this shift, whereas the CFM naturally extrapolates the earlier, pre-intervention relationships.

5.5 Formal CFM:OAM Comparison

Traditional sequential Bayesian model monitoring (West and Harrison, 1997, Chapter 11) defines one summary numerical evaluation of the departure of the observed data from expectations under the CFM relative to the data-respecting OAM. This simply involves sequential updates of the relative model probabilities based on the ratio of time t marginal likelihoods of Section 3.4. As the models differ only in the lower discount factor at $t = 1990$, this provides an additional, quantitative assessment of the impact of the intervention.

Figure 7 displays the resulting trajectory of the probability on the OAM relative to the CFM based on equal probabilities at 1990 (until which time the models are, of course, the same). The increased uncertainty under the OAM just after the intervention leads to lower probabilities for one or two years. In 1993, however, several European countries experienced recessionary effects with lower GDP and in which Germany had its only year of negative GDP growth from 1961 to 2003.

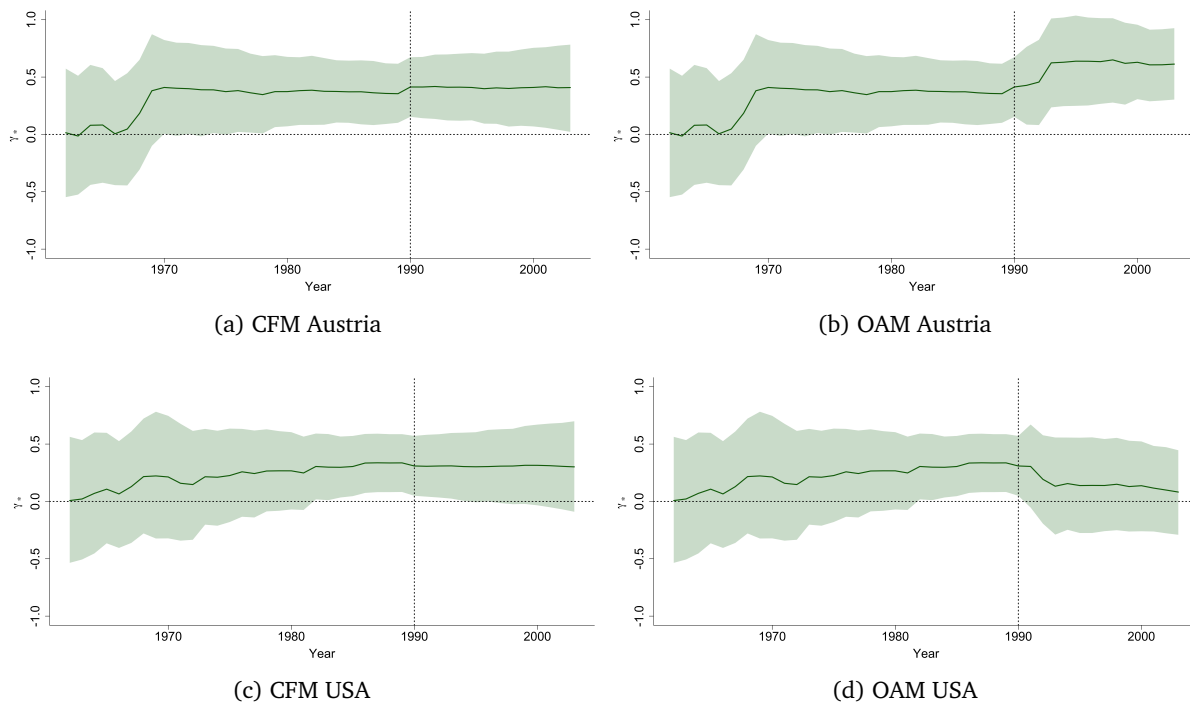


Figure 6: GDP example: Trajectories of simultaneous coefficients of Germany on Austria and USA.

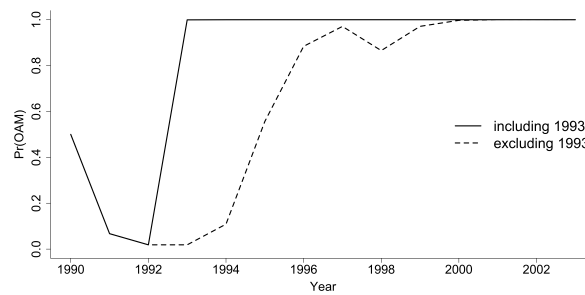


Figure 7: Trajectory of post-1990 accumulating evidence in favour of the OAM over the CFM.

These departures from past trends are not anticipated by the CFM and the probability on the OAM shoots up to high levels in 1993 and thereafter. This large impact is heavily influenced by series-specific contributions from Germany, Spain and Portugal, in particular. Throughout the rest of the post-intervention period, only 1998 contributes positively in favour of CFM, attributable largely to anomalous GDP growth for Norway that year. A rerun of this computation ignoring the evidence from 1993 is also displayed. This shows the OAM increasingly favoured as the 1990s progress, but high confidence in the OAM compared to the CFM is reached only in the late 1990s.

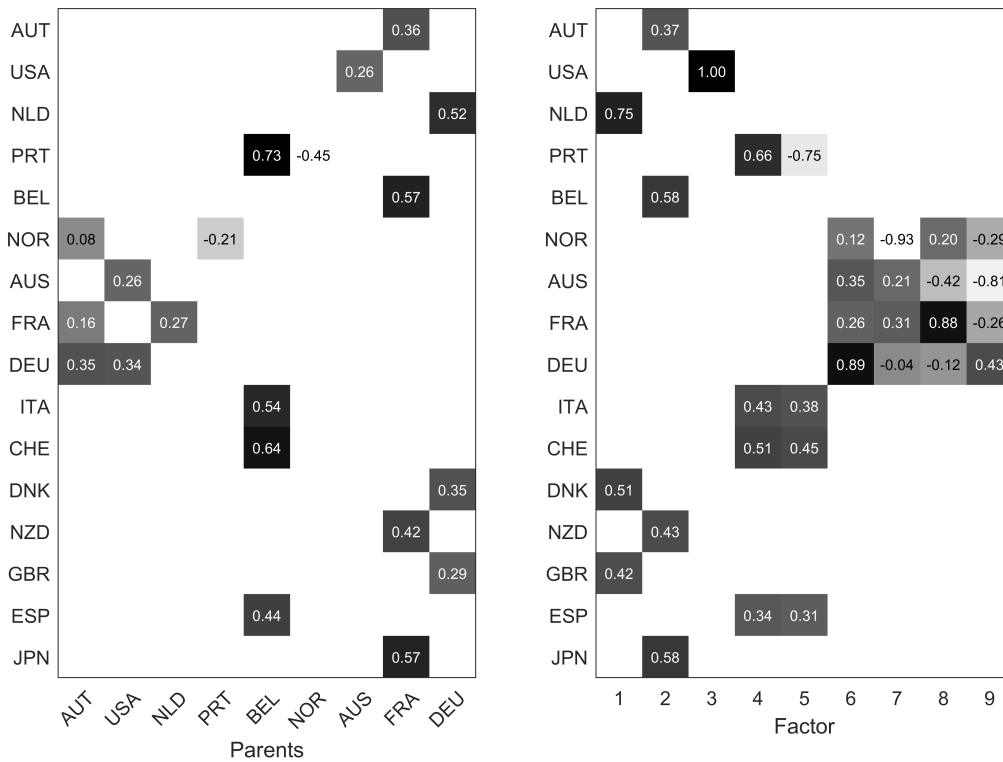
5.6 Sparse Dynamic Factor Model from SGDLM for GDP Series

Selected summaries of the implied dynamic factor structure of Section 3.2 provide further insights. In each year t , inference on Γ_t defines inference on the factor loadings, singular values and scores $\mathbf{L}_t, \mathbf{D}_t, \mathbf{S}_t$, respectively, together with the implied factor process η_t . While the non-zero elements in $\Gamma_t, \mathbf{L}_t, \mathbf{S}_t$ are time-varying, the SGDLM graph implies fixed patterns of sparsity in each; this aids in interpretation of the factors. In this example, each Γ_t has 7 zero columns, $\text{rank}(\Gamma) = 9$, and there are 5 common parental sets.

Factor sparsity patterns are exemplified in Figure 8, a snapshot at $t = 1989$. These are summaries from the OAM analysis, which of course subsumes the CFM analysis prior to the intervention at 1990. The zero/non-zero factor pattern in each \mathbf{S}_t relates to the 5 common parental sets. The specific ordering of factors is as follows: (a) $\mathcal{P}_1 = \{\text{DEU}\}$ alone defines factor 1; (b) $\mathcal{P}_2 = \{\text{FRA}\}$ alone defines factor 2; (c) $\mathcal{P}_3 = \{\text{AUS}\}$ alone defines factor 3; (d) $\mathcal{P}_4 = \{\text{BEL}, \text{NOR}\}$ represents series inter-dependencies reflected in factors 4 and 5; (e) $\mathcal{P}_5 = \{\text{AUT}, \text{USA}, \text{NLD}, \text{PRT}\}$ represents series inter-dependencies reflected in factors 6,7,8 and 9. Values of the non-zero elements of the factor matrices are computed based on the on-line, filtered means of the Γ_t over time, projected to factors via the SVD. Appendix E has corresponding figures for $t = 1990$ and 1993; these show variation at and just after the intervention, and then at the main drop in DEU GDP in 1993.

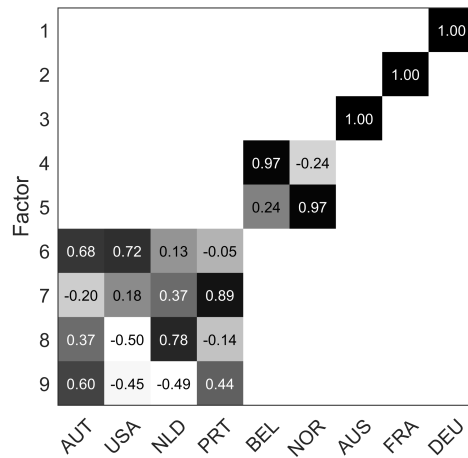
Inherent ambiguities in factor signs, ordering and matching between time points are resolved as follows. “Permuting factors” at each t refers to applying a chosen permutation to the rows of \mathbf{S}_t , the diagonal of \mathbf{D}_t and the columns of \mathbf{L}_t generated from the SVD. The first step is to permute factors if needed to match the zero/non-zero pattern of \mathbf{S}_t with a chosen reference pattern; the latter is arbitrary, here chosen simply for clarity and aesthetics of resulting figures. The second step multiplies each row of \mathbf{S}_t and the corresponding column of \mathbf{L}_t by ± 1 so that the largest element in absolute value in the row is positive. The third step applies to each parental set. In each \mathcal{P}_h this permutes the p_h factors in order so that the first has the largest score in the relevant row of \mathbf{S}_t from among this subset of p_h series in \mathcal{P}_h , the second has the largest ignoring the first, and so forth. These second and third steps relate to ordering of factors “founder” variables in [Carvalho et al. \(2008\)](#), extended and referred to as “pivot” variables in [Frühwirth-Schnatter et al. \(2024\)](#).

Figure 9 shows estimated trajectories of 4 selected factors, again based on the on-line, filtered means of the Γ_t over time projected to factors. The initial several years represent a learning phase as the SGDLM analysis adapts to incoming data, but once into the early 1970s the nature of the factors becomes clear as accruing data informs on state vectors and volatilities. The 4 factors chosen here highlight interpretation in the macroeconomic setting. In addition to the behaviour of DEU



(a) Regression matrix $\Gamma_t: t = 1989$

(b) Loadings matrix $L_t: t = 1989$



(c) Scores matrix $S_t: t = 1989$

Figure 8: GDP example: Sparsity patterns (white= 0) and point estimates (shading numbers) of non-zero values in estimated matrices (a) Γ_t , (b) L_t and (c) S_t at $t = 1989$. The 7 final columns of Γ_t are zero and so are omitted.

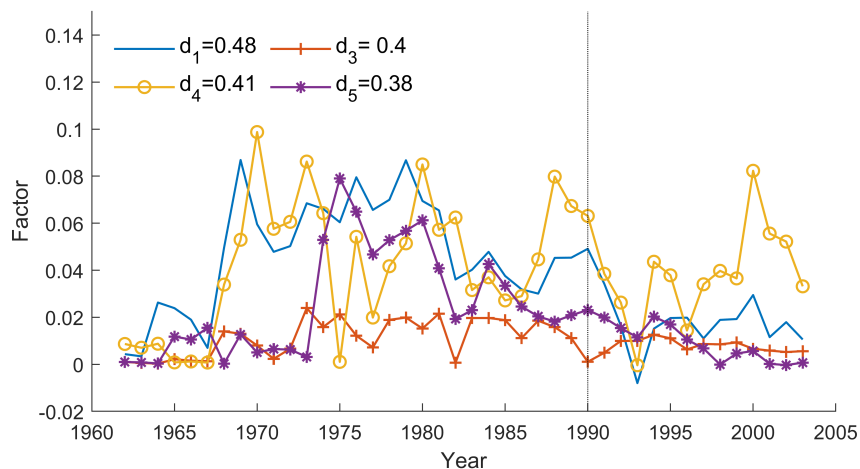


Figure 9: GDP example: Trajectories of 4 selected simultaneous factors η_{jt} for $j = 1, 3, 4, 5$, indexed by corresponding singular values in the defining SVDs. Singular values shown are the averages of the plug-in estimates over the years 1975–2003, giving a broad indication of relative contributions to the set of series. Coupled with that, the factors are evaluated and shown on the absolute $\Delta \log \$GDP$ scale, so are directly comparable in terms of their contributions to the description of variations in the set of series over the time period.

factor 1 over 1991–1993, some of the other factors show distinct drops over that period. There is inherent contextual confounding of the impact of German reunification with other global economy events in the early 1990s that contributed to Western economy recessions, and the full set of factors reflect complex cross-series relationships arising as a result over those years. That said, we note some illuminating details evident in the patterns of estimated factor evolution over time.

Factor 1 is the DEU founded factor, showing the marked drop in the early 1990s, especially marked in 1993, post-intervention. Factor 3 is the AUS founded factor, showing marked stability over the full time period and no serious evidence of impact of the 1990 reunification intervention. Factor 4 is one of the two BEL-NOR founded factors, showing substantial volatility over the years and then a profound drop in the early 1990s reflecting major GDP deflation in EU economies generally– and those countries loaded on this factor, in particular– over these years. Factor 5 is the second of the 2 BEL-NOR founded factors, loaded on the same set of countries. In contrast to factor 4, this NOR-dominated factor is very stable indeed over the pre- and post-reunification period, showing no noticeable impact of the intervention. It is clearly a stable, NOR-dominated factor that underlies aspects of the covariation over time in the GDP of other countries, but unrelated to the core DEU-EU event of primary interest. A notable reflection of this, and the nature of factor 5, is the large estimated increase in 1974–1976; this is at and immediately following the global oil crisis that substantially inflated the market pricing of crude oil– and resulting petroleum products– to the benefit of GDP in what was then one of the premier producers and suppliers of crude oil. This is a nice, interpretable factor in distinguishing patterns in multi-national GDP that can be directly interpreted in terms of historical events of global economic importance.

Analysis here takes the SVD-based singular factors based on plug-in filtered posterior means of the Γ_t . We note that, if of interest, the same factor evaluation and permutation analysis can be applied to each Γ_t in the filtered posterior Monte Carlo sample, with resulting summaries of full posterior uncertainties. While not a primary interest in the current paper, this is relevant to future applications of these models. Examples of filtered trajectories over time for these 4 selected factors based on the full Monte Carlo samples are shown in Appendix E.

6 Summary Comments

SGDLMs are increasingly used in applications such as forecasting for decision analysis in financial time series. Their broader utility in other areas of time series is based on the inherent flexibility, parsimony and scalability with series dimension. Modelling flexibility is due to: (i) sensitive modelling of each of the decoupled univariate series separately, enabling use of relevant exogenous and simultaneous predictors customised to each series; and (ii) sensitive recoupling across the set of series through the simultaneous parental structure. This flexibility is enhanced by the inherent sequential model specification and Bayesian analysis that admits, evaluates and exploits time-variation in model parameters. Parsimony is enhanced by the decouple/recouple perspective and the use of underlying sparse graphical structure for cross-series relationships as part of that. Scalability is enabled— computational loads scale linearly in the number of univariate time series— as a result of the decouple/recouple modelling strategy.

The graphical and factor model connections introduced here— linking intimately to the graph theory underlying SGDLMs and related linear algebra— define nice connections between what have been regarded as incompatible approaches to modelling multivariate dependencies. Sparse factor models have zeros in covariance matrices while sparse graphical models have zeros in precision matrices; these are generally incompatible (though see [Yoshida and West, 2010](#) for one prior existence proof of compatibility). The general graphical structure of SGDLMs induces implicit factor structure, so providing an opening for new developments in factor modelling generally as well as specific to time series.

A main motivation and goal for the developments here is the extension of SGDLM methodology to settings of counterfactual forecasting driven by putatively causal interests. The existing methodology has now been extended to admit missing data on some of the univariate time series after a defined intervention time point, beyond which the designated experimental series are predicted based on the rest within the continuing evolution of the SGDLM. Bayesian computations— relying only on simple, direct simulation— remain sequential and efficient, exploit theory underlying the model structure, and neatly extend existing methods.

This paper has explored these aspects of theory and methodology in the context of a given parental structure underlying the the SGDLM. Exploring analyses against several graphs, chosen on empirical or contextual bases, is routine. Considering the graph as an underlying uncertain parameter defines research questions of dynamic variable selection and model uncertainty, with open research challenges. While this is not a perspective we would adopt in some applications— where identifying predictively useful graphical structures modulo specific goals is primary— some of

the existing Bayesian approaches to variable selection and model uncertainty analysis in time series and allied areas (e.g. [Jones et al., 2005](#); [Hans et al., 2007](#); [Nakajima and West, 2013a](#); [Lavine et al., 2021](#)) are certainly of interest. Some applications may involve specific decision goals– including potentially some applications in causal analysis where the inferences feed into actionable decisions. In such settings, the parental/graphical structure selection question might best be embedded in model weightings relative to historical and near-term expected decision outcomes using ideas from Bayesian predictive decision synthesis ([Tallman and West, 2023, 2024](#)).

Acknowledgements

The authors acknowledge useful discussions with Kevin Li and Graham Tierney in the formative stages of the research presented here. Lutz Gruber’s R code for SGDLMS ([Gruber, 2018](#)) was used and modified for aspects of the analysis.

References

- Abadie, A., A. Diamond, and J. Hainmueller (2015). Comparative politics and the synthetic control method. *American Journal of Political Science* 59, 495–510.
- Abadie, A. and J. Gardeazabal (2003). The economic costs of conflict: A case study of the Basque Country. *American Economic Review* 93, 113–132.
- Antonelli, J. and B. Beck (2023). Heterogeneous causal effects of neighbourhood policing in New York City with staggered adoption of the policy. *Journal of the Royal Statistical Society: Series A (Statistics in Society)* 186, 772–787.
- Bañbura, M., D. Giannone, and L. Reichlin (2010). Large Bayesian vector autoregressions. *Journal of Applied Econometrics* 25, 71–92.
- Bolfarine, H., C. M. Carvalho, H. F. Lopes, and J. S. Murray (2024). Decoupling shrinkage and selection in Gaussian linear factor analysis. *Bayesian Analysis* 19, 181–203.
- Brodersen, K. H., F. Gallusser, J. Koehler, N. Remy, and S. L. Scott (2015). Inferring causal impact using Bayesian structural time-series models. *The Annals of Applied Statistics* 9, 247–274.
- Carvalho, C. M., J. E. Lucas, Q. Wang, J. Chang, J. R. Nevins, and M. West (2008). High-dimensional sparse factor modelling– Applications in gene expression genomics. *Journal of the American Statistical Association* 103, 1438–1456.
- Crawford, L., S. R. Flaxman, D. E. Runcie, and M. West (2019). Variable prioritization in nonlinear black box methods: A genetic association case study. *Annals of Applied Statistics* 13, 958–989.
- Cvetkovic, D., M. Doob, and H. Sachs (1980). *Spectra of Graphs: Theory and Application*. New York: Academic Press.
- Fang, Z., S. Zhu, J. Zhang, Y. Liu, Z. Chen, and Y. He (2024). On low-rank directed acyclic graphs and causal structure learning. *IEEE Transactions on Neural Networks and Learning Systems* 35, 4924–4937.

- Frühwirth-Schnatter, S., D. Hosszejni, and H. F. Lopes (2024). Sparse Bayesian factor analysis when the number of factors is unknown. *Bayesian Analysis*.
- Griveau-Billion, T. and B. Calderhead (2021). Efficient computation of mean reverting portfolios using cyclical coordinate descent. *Quantitative Finance* 21, 673–684.
- Gruber, L. F. (2018). *GPU-accelerated software for online learning of the simultaneous graphical DLM*. Software: github.com/lutzgruber/gpuSGDLM.
- Gruber, L. F. and M. West (2016). GPU-accelerated Bayesian learning and forecasting in simultaneous graphical dynamic linear models. *Bayesian Analysis* 11, 125–149.
- Gruber, L. F. and M. West (2017). Bayesian forecasting and scalable multivariate volatility analysis using simultaneous graphical dynamic linear models. *Econometrics and Statistics* 3, 3–22.
- Hans, C., A. Dobra, and M. West (2007). Shotgun stochastic search in regression with many predictors. *Journal of the American Statistical Association* 102, 507–516.
- Horn, R. and C. Johnson (2012). *Matrix Analysis* (2nd ed.). Cambridge University Press.
- Jones, B., A. Dobra, C. M. Carvalho, C. Hans, C. Carter, and M. West (2005). Experiments in stochastic computation for high-dimensional graphical models. *Statistical Science* 20, 388–400.
- Jones, B. and M. West (2005). Covariance decomposition in undirected Gaussian graphical models. *Biometrika* 92, 779–786.
- Kaufmann, S. and C. Schumacher (2019). Bayesian estimation of sparse dynamic factor models with order-independent and ex-post mode identification. *Journal of Econometrics* 210, 116–134.
- Klößner, S., A. Kaul, G. Pfeifer, and M. Schieler (2018). Comparative politics and the synthetic control method revisited: A note on Abadie et al. (2015). *Swiss Journal of Economics and Statistics* 154, 11.
- Koop, G. and D. Korobilis (2010). Bayesian multivariate time series methods for empirical macroeconomics. *Foundations and Trends in Econometrics* 3, 267–358.
- Koop, G. and D. Korobilis (2013). Large time-varying parameter VARs. *Journal of Econometrics* 177, 185–198.
- Kyakutwika, N. (2023). *SGDLM in python*. Software: github.com/nelsonkyakutwika/SGDLM.
- Kyakutwika, N. and B. Bartlett (2024). Bayesian forecasting of stock returns on the JSE using simultaneous graphical dynamic linear models. *Investment Analysts Journal*, 1–20.
- Lavine, I., A. J. Cron, and M. West (2022). Bayesian computation in dynamic latent factor models. *Journal of Computational and Graphical Statistics* 31, 651–665.
- Lavine, I., M. Lindon, and M. West (2021). Adaptive variable selection for sequential prediction in multivariate dynamic models. *Bayesian Analysis* 16, 1059–1083.
- Li, K., G. Tierney, C. Hellmayr, and M. West (2024). Compositional dynamic modelling for causal prediction in multivariate time series. *Submitted for publication*. arXiv:2406.02320.
- Lopes, H. F. and C. M. Carvalho (2007). Factor stochastic volatility with time varying loadings and Markov switching regimes. *Journal of Statistical Planning and Inference* 137, 3082–3091.

- Lopes, H. F., R. E. McCulloch, and R. S. Tsay (2022). Parsimony inducing priors for large scale state–space models. *Journal of Econometrics* 230, 39–61.
- Marimont, R. B. (1969). System connectivity and matrix properties. *The Bulletin of Mathematical Biophysics* 31, 255–274.
- Menchetti, F. and I. Bojinov (2022). Estimating the effectiveness of permanent price reductions for competing products using multivariate Bayesian structural time series models. *The Annals of Applied Statistics* 16, 414–435.
- Nakajima, J. and M. West (2013a). Bayesian analysis of latent threshold dynamic models. *Journal of Business and Economic Statistics* 31, 151–164.
- Nakajima, J. and M. West (2013b). Bayesian dynamic factor models: Latent threshold approach. *Journal of Financial Econometrics* 11, 116–153.
- Nakajima, J. and M. West (2015). Dynamic network signal processing using latent threshold models. *Digital Signal Processing* 47, 6–15.
- Nakajima, J. and M. West (2017). Dynamics and sparsity in latent threshold factor models: A study in multivariate EEG signal processing. *Brazilian Journal of Probability and Statistics* 31, 701–731.
- Pang, X., L. Liu, and Y. Xu (2022). A Bayesian alternative to synthetic control for comparative case studies. *Political Analysis* 30, 269–288.
- Prado, R., M. A. R. Ferreira, and M. West (2021). *Time Series: Modeling, Computation & Inference* (2nd ed.). Chapman & Hall/CRC Press.
- Primiceri, G. E. (2005). Time varying structural vector autoregressions and monetary policy. *Review of Economic Studies* 72, 821–852.
- Simovici, D. A. and C. Djeraba (2014). Spectral properties of matrices. In *Mathematical Tools for Data Mining: Set Theory, Partial Orders, Combinatorics*, pp. 347–397. Springer.
- Tallman, E. and M. West (2023). Bayesian predictive decision synthesis. *Journal of the Royal Statistical Society (Ser. B)* 86, 340–363.
- Tallman, E. and M. West (2024). Predictive decision synthesis for portfolios: Betting on better models. In S. Mazur and P. Österhol (Eds.), *Recent Developments in Bayesian Econometrics and Their Applications*. Springer. arXiv:2405.01598.
- Tiao, G. C. and R. S. Tsay (1989). Model specification in multivariate time series. *Journal of the Royal Statistical Society: Series B (Statistical Methodology)* 51, 157–195.
- Tierney, G., C. Hellmayr, K. Li, G. Barkimer, and M. West (2024). Multivariate Bayesian dynamic modeling for causal prediction. *Bayesian Analysis*. arXiv:2302.03200.
- West, M. (2020). Bayesian forecasting of multivariate time series: Scalability, structure uncertainty and decisions (with discussion). *Annals of the Institute of Statistical Mathematics* 72, 1–44.
- West, M. and P. J. Harrison (1986). Monitoring and adaptation in Bayesian forecasting models. *Journal of the American Statistical Association* 81, 741–750.

West, M. and P. J. Harrison (1997). *Bayesian Forecasting and Dynamic Models* (2nd ed.). Springer.

Xu, C. (2024). *The DYNAMICLINEAR Procedure*. SAS: Econometrics Software.

Yoshida, R. and M. West (2010). Bayesian learning in sparse graphical factor models via annealed entropy. *Journal of Machine Learning Research* 11, 1771–1798.

Zhao, Z. Y., M. Xie, and M. West (2016). Dynamic dependence networks: Financial time series forecasting and portfolio decisions (with discussion). *Applied Stochastic Models in Business and Industry* 32, 311–339. arXiv:1606.08339.

Zhou, X., J. Nakajima, and M. West (2014). Bayesian forecasting and portfolio decisions using dynamic dependent sparse factor models. *International Journal of Forecasting* 30, 963–980.

Additional Appendices and Supplementary Material

Dynamic Graphical Models: Theory, Structure and Counterfactual Forecasting

Luke Vrotsos & Mike West

Appendix A Summary of Filtering and Forecasting in SGDLMs

Analysis is sequential over time, summarised here in the time $t - 1$ to t forecast-update-evolve steps that are then repeated into the future. Full details are in [Gruber and West \(2016, 2017\)](#).

Decoupled post-forecasting prior for updating at time t . Independently across series and conditional on \mathcal{D}_{t-1} , the inferences on the series j state vector and precision in each univariate model of eqn. (2) for use in updating based on time t observations are constrained to be of conjugate normal-gamma form,

$$\text{p.d.f. } p_{j,t-1}(\boldsymbol{\theta}_{jt}, \lambda_{jt} | \mathcal{D}_{t-1}) : \quad (\boldsymbol{\theta}_{jt}, \lambda_{jt} | \mathcal{D}_{t-1}) \sim \text{NG}(\mathbf{m}_{jt}^*, \mathbf{M}_{jt}^*, n_{jt}^*, s_{jt}^*), \quad j = 1 : q, \quad (4)$$

with all parameters superscripted $*$ known at time $t - 1$. The NG notation summarises $\boldsymbol{\theta}_{jt} | \lambda_{jt} \sim \text{N}(\mathbf{m}_{jt}^*, \mathbf{M}_{jt}^* / (s_{jt}^* \lambda_{jt}))$ and $\lambda_{jt} \sim \text{G}(n_{jt}^* / 2, n_{jt}^* s_{jt}^* / 2)$ with n_{jt}^* degrees of freedom and mean $1 / s_{jt}^*$. The $\boldsymbol{\theta}_{jt}$ margin is multivariate T with n_{jt}^* degrees of freedom, mode \mathbf{m}_{jt}^* and scale matrix \mathbf{M}_{jt}^* . $(\boldsymbol{\theta}_{jt}, \lambda_{jt} | \mathcal{D}_{t-1})$. With $\boldsymbol{\Theta}_t = [\boldsymbol{\theta}_{1t}, \dots, \boldsymbol{\theta}_{qt}]$ and $\boldsymbol{\Lambda}_t = \text{diag}(\lambda_{1t}, \dots, \lambda_{qt})$, the joint prior over series is

$$p_t(\boldsymbol{\Theta}_t, \boldsymbol{\Lambda}_t | \mathcal{D}_{t-1}) = \prod_{j=1:q} p_{jt}(\boldsymbol{\theta}_{jt}, \lambda_{jt} | \mathcal{D}_{t-1}). \quad (5)$$

Update to posterior at time t and recoupling across models. In each of the decoupled models separately, standard conjugate posteriors are

$$\text{p.d.f. } \tilde{p}_{jt}(\boldsymbol{\theta}_{jt}, \lambda_{jt} | \mathcal{D}_t) : \quad (\boldsymbol{\theta}_{jt}, \lambda_{jt} | \mathcal{D}_{t-1}) \sim \text{NG}(\tilde{\mathbf{m}}_{jt}, \tilde{\mathbf{M}}_{jt}, \tilde{n}_{jt}, \tilde{s}_{jt}), \quad j = 1 : q, \quad (6)$$

with defining parameters based on the usual DLM updating equations. These are $\tilde{\mathbf{m}}_{jt} = \mathbf{m}_{jt}^* + \mathbf{a}_{jt} e_{jt}$, $\tilde{\mathbf{M}}_{jt} = (\mathbf{M}_{jt}^* - \mathbf{a}_{jt} \mathbf{a}_{jt}' q_{jt}) z_{jt}$, $\tilde{n}_{jt} = n_{jt}^* + 1$ and $\tilde{s}_{jt} = z_{jt} s_{jt}^*$ based on the point forecast error $e_{jt} = y_{jt} - \mathbf{F}_{jt}' \mathbf{m}_{jt}^*$, the adaptive coefficient vector $\mathbf{a}_{jt} = \mathbf{M}_{jt}^* \mathbf{F}_{jt} / q_{jt}$ where the 1-step forecast variance factor q_t is defined above, and volatility update factor $z_{jt} = (n_{jt}^* + e_{jt}^2 / q_{jt}) / (n_{jt}^* + 1)$.

The exact joint posterior is

$$p_t(\boldsymbol{\Theta}_t, \boldsymbol{\Lambda}_t | \mathcal{D}_t) \propto |\mathbf{I} - \boldsymbol{\Gamma}_t|_+ \prod_{j=1:q} \tilde{p}_{jt}(\boldsymbol{\theta}_{jt}, \lambda_{jt} | \mathcal{D}_t) \propto |\mathbf{I} - \boldsymbol{\Gamma}_t|_+ \tilde{p}_t(\boldsymbol{\Theta}_t, \boldsymbol{\Lambda}_t | \mathcal{D}_t). \quad (7)$$

where $\tilde{p}_t(\boldsymbol{\Theta}_t, \boldsymbol{\Lambda}_t | \mathcal{D}_t) = \prod_{j=1:q} \tilde{p}_{jt}(\boldsymbol{\theta}_{jt}, \lambda_{jt} | \mathcal{D}_t)$, referred to as the naive posterior, defines what is typically an excellent approximation to $p_t(\boldsymbol{\Theta}_t, \boldsymbol{\Lambda}_t | \mathcal{D}_t)$.

The absolute value of the determinant of $\mathbf{I} - \mathbf{\Gamma}_t$ *recouples* the naive conjugate posteriors, accounting for cross-series dependencies. Independent Monte Carlo samples from each of the $\tilde{p}_{jt}(\cdot|\cdot)$ are importance-weighted by the determinant term, defining importance sampling (IS) of the exact posterior $p(\boldsymbol{\Theta}_t, \boldsymbol{\Lambda}_t|\mathcal{D}_t)$. The posterior is summarised by the IS sample and weights $\mathcal{S}_t = \{\boldsymbol{\Theta}_t^r, \boldsymbol{\Lambda}_t^r, w_t^r\}_{r=1:R}$ where R is the number of Monte Carlo replicates, and each sampled pair $\boldsymbol{\Theta}_t^r, \boldsymbol{\Lambda}_t^r$ pair has importance weight w_t^r (summing to 1 over $r = 1 : R$).

Forecasting ahead at time t . Direct simulation enables forecasting from the full predictive distribution over one or more steps ahead. For replicates $r = 1 : R$, (a) sample one parameter set $\boldsymbol{\Theta}_t^r, \boldsymbol{\Lambda}_t^r$ from \mathcal{S}_t according to the IS weights; (b) conditional on this draw, sample a corresponding pair $\boldsymbol{\Theta}_{t+1}^r, \boldsymbol{\Lambda}_{t+1}^r$ from the evolution equations of the SGDLM, and recurse into the future to $k > 1$ steps ahead as required; (c) at each $h = 1 : k$, compute the implied normal parameters $(\boldsymbol{\alpha}_{t+h}^r, \boldsymbol{\Omega}_{t+h}^r)$ as defined in Section 3.1, then draw \mathbf{y}_{t+h}^r from that conditional normal distribution. The result is a draw from the full predictive distribution $p(\mathbf{y}_{t+1}, \dots, \mathbf{y}_{t+k}|\mathcal{D}_t)$.

Decoupling for evolution to time $t + 1$. The posterior is decoupled into a product of conjugate forms based on a mean-field, reverse variational Bayes (VB) approach. This emulates the exact posterior by the product form $q_t(\boldsymbol{\Theta}_t, \boldsymbol{\Lambda}_t|\mathcal{D}_t) = \prod_{j=1:q} q_{jt}(\boldsymbol{\theta}_{jt}, \lambda_{jt}|\mathcal{D}_t)$ with components

$$\text{p.d.f. } q_{jt}(\boldsymbol{\theta}_{jt}, \lambda_{jt}|\mathcal{D}_t) : \quad (\boldsymbol{\theta}_{jt}, \lambda_{jt}|\mathcal{D}_t) \sim \text{NG}(\mathbf{m}_{jt}, \mathbf{M}_{jt}, n_{jt}, s_{jt}), \quad j = 1 : q. \quad (8)$$

The parameters of each NG component are evaluated to minimise the Kullback-Leibler divergence of the product form $q(\cdot|\cdot)$ from $p(\cdot|\cdot)$, and are trivially calculated.

Evolution to time $t + 1$. The evolution of the $\boldsymbol{\theta}_{jt}, \lambda_{jt}$ to $\boldsymbol{\theta}_{j,t+1}, \lambda_{j,t+1}$, independently in each univariate DLM, follows standard univariate DLM theory. This involves a volatility discount factor $\beta \in (0, 1]$ and the state innovation variance matrix $\mathbf{W}_{j,t+1}$ for the model eqn. (2) at time $t + 1$. The latter is specified using a block discount strategy (West and Harrison, 1997, chap. 6); $\mathbf{W}_{j,t+1}$ is block diagonal with 2 blocks corresponding to the partition of $\boldsymbol{\theta}_{jt}$ in the model eqn. (2), i.e., $\boldsymbol{\theta}_{jt} = (\boldsymbol{\phi}_{jt}, \boldsymbol{\gamma}_{jt})'$. The blocks of $\mathbf{W}_{j,t+1}$ are variance matrices of the evolution innovations on the dynamic regression parameters (i) $\boldsymbol{\phi}_{jt}$, of any trends and exogenous predictors, and (ii) $\boldsymbol{\gamma}_{jt}$, of the parental predictors. Discount factors $\delta_\phi, \delta_\gamma$ define the variance matrix blocks, and allow differing degrees of discounting on the 2 subvectors. Note that the GDP example in the paper adopts the specification that $\delta_\phi = \delta_\gamma = \delta$. The resulting prior for time $t + 1$ maintains the conjugate form of eqns. (4,5), with parameters evolved to $\mathbf{m}_{j,t+1}^* = \mathbf{G}_{j,t+1}\mathbf{m}_{jt}$, $\mathbf{M}_{j,t+1}^* = \mathbf{G}_{j,t+1}\mathbf{M}_{jt}^*\mathbf{G}_{j,t+1}' + \mathbf{W}_{j,t+1}$, $n_{j,t+1}^* = \beta_j n_{jt}$ and $s_{j,t+1}^* = s_{jt}$. This completes the update-forecast-evolve steps, and analysis moves to the next time period.

Appendix B Eigenstructure of Simultaneous System

Refer to the summary theory in Section 2.1. Whatever the sparsity pattern of $\mathbf{\Gamma}$, the matrix $\mathbf{I} - \mathbf{\Gamma}$ is invertible unless elements of $\mathbf{\Gamma}$ are subject to pathological deterministic constraints. In the statistical setting with continuous priors and posteriors over the non-zero elements of $\mathbf{\Gamma}$, invertibility holds with probability one since the eigenvalues of $\mathbf{I} - \mathbf{\Gamma}$ will be non-zero with probability one.

Write $\mathbf{g} = \{g_1, \dots, g_q\}$ for the (real or complex) eigenvalues of Γ . In applications, posteriors over Γ will often favour regions where $|g_i| < 1$ for all $i = 1 : q$. The insights into spillover of Section 2.1 are then implied as $|\Gamma| < 1$. If, for example, the y_i are all on the same scale, it is natural to expect that $\sum_{j \in sp(i)} |\gamma_{ij}| < 1$ (i.e., expecting “shrinkage to the mean” in the univariate conditional models) which ensures all $|g_i| < 1$ by the Gershgorin disc theorem (Horn and Johnson, 2012, Chapter 6). Empirical studies typically give estimated or simulated parameters with $\max(|g_i|) < 1$. Theoretically, however, some of the eigenvalues may lie outside the unit circle, but nothing changes in terms of the implied joint model. If desired, Bayesian analyses of SGDLMs can be simply modified to reject cases in which one or more eigenvalues exceeds 1 in absolute value. This can be formally incorporated as a constraint in priors, and imposed in weightings or accept/reject steps in the Monte Carlo (importance and/or MCMC) posterior analyses.

Some general points about the eigenstructure of Γ follow from the corresponding directed graph. A *cycle* is a path in the directed graph corresponding to Γ that begins and ends at the same node, following the direction of the arrows, with an *order* given by the number of nodes in the cycle. Let r be the greatest number of nodes included in any collection of disjoint cycles in the directed graph. The following results hold.

- Γ has at least $q - r$ zero eigenvalues, as $(-\delta)^{q-r}$ is a factor of the characteristic polynomial.
- For acyclic graphs, $r = 0$ and $g_i = 0$ for all $i = 1 : q$ (Cvetkovic et al., 1980, Chapter 3). In such a case, the order of the series can be permuted so that the resulting Γ is strictly lower triangular with zero diagonal elements, and the simultaneous system reduces to a compositional factorization of $p(\mathbf{y})$.
- If Γ has at least one cycle and all cycles are of even order, then all non-zero eigenvalues of Γ occur in pairs $\pm\lambda$ (Marimont, 1969, Theorem 5); when this condition holds for odd q , at least one of the g_i is 0.

Appendix C Marginal Likelihood Calculation in SGDLMs

Further details on the evaluation of 1-step ahead forecast density functions for marginal likelihoods are detailed here. For clarity here, the notation initially drops the t index and conditioning information set \mathcal{D}_{t-1} . Thus, in general form the p.d.f. of interest is

$$p(\mathbf{y}) = \int |\mathbf{I} - \Gamma|_+ \prod_{j=1}^q p_j(y_j | \mathbf{y}_{sp(j)}, \boldsymbol{\theta}_j, \lambda_j) p_j(\boldsymbol{\theta}_j, \lambda_j) d\boldsymbol{\Theta} d\boldsymbol{\Lambda}$$

in which the q terms in the p.d.f. product are normal linear regressions with conjugate NG priors.

Sampling from the prior $p(\Gamma)$. Further simplification emerges by marginalizing out the ϕ_j, λ_j terms to give

$$p(\mathbf{y}) = \int |\mathbf{I} - \Gamma|_+ \prod_{j=1}^q p_j(y_j | \mathbf{y}_{sp(j)}, \boldsymbol{\gamma}_j) p_j(\boldsymbol{\gamma}_j) d\Gamma \quad (9)$$

where each $p_j(\gamma_j)$ is the p.d.f. of the marginal multivariate T prior for the simultaneous parental subvector in series j .

This suggests drawing a random sample $\mathbf{\Gamma}^i \sim p(\mathbf{\Gamma})$, ($i = 1 : M$), from the set of independent T priors, and then defining the Monte Carlo estimate

$$\hat{p}(\mathbf{y}) = M^{-1} \sum_{i=1}^M |\mathbf{I} - \mathbf{\Gamma}^i|_+ f(\mathbf{y}|\mathbf{\Gamma}^i)$$

where $f(\mathbf{y}|\mathbf{\Gamma})$ is the product of the univariate p.d.f.s for each series. A drawback of sampling from the prior is that the $\mathbf{\Gamma}$ draws do not take into account the observed \mathbf{y} , so may be values that are in fact unlikely under the posterior.

Sampling from the posterior $p(\mathbf{\Gamma}|\mathbf{y})$. In order to produce more-probable draws of the γ_j , reorganisation of the integrand in eqn. (9) gives

$$p(\mathbf{y}) = f(\mathbf{y}) \int |\mathbf{I} - \mathbf{\Gamma}|_+ \prod_{j=1}^q p(\gamma_j|y_j, \mathbf{y}_{sp(j)}) d\mathbf{\Gamma}$$

where the terms in the product in the integrand are the p.d.f.s of the marginal *posterior* T distributions for parental coefficient subvectors in the set of series, and $f(\mathbf{y}) = \prod_{j=1}^q p_j(y_j)$ is the product of marginal predictive densities.

The Monte Carlo approach summarised in Section 3.4 is based on posterior sampling: draw a random sample $\mathbf{\Gamma}^i \sim p(\mathbf{\Gamma}|\mathbf{y})$, ($r = 1 : R$), to define the estimate

$$\bar{p}(\mathbf{y}) = R^{-1} f(\mathbf{y}) \sum_{r=1}^R |\mathbf{I} - \mathbf{\Gamma}^r|_+. \quad (10)$$

Efficiency gain from posterior sampling. For $\mathbf{\Gamma} \sim p(\mathbf{\Gamma})$, let $\alpha = f(\mathbf{y}|\mathbf{\Gamma})$ and $\beta = |\mathbf{I} - \mathbf{\Gamma}|_+^2 f(\mathbf{y}|\mathbf{\Gamma})$. The variances of the two Monte Carlo estimators are given by

$$RV[\hat{p}(\mathbf{y})] = \int |\mathbf{I} - \mathbf{\Gamma}|_+^2 f(\mathbf{y}|\mathbf{\Gamma})^2 p(\mathbf{\Gamma}) d\mathbf{\Gamma} + p(\mathbf{y})^2 = E[\alpha\beta] + p(\mathbf{y})^2,$$

$$RV[\bar{p}(\mathbf{y})] = f(\mathbf{y}) \int |\mathbf{I} - \mathbf{\Gamma}|_+^2 f(\mathbf{y}|\mathbf{\Gamma}) p(\mathbf{\Gamma}) d\mathbf{\Gamma} + p(\mathbf{y})^2 = E[\alpha]E[\beta] + p(\mathbf{y})^2.$$

Thus $M\{V[\hat{p}(\mathbf{y})] - V[\bar{p}(\mathbf{y})]\} = E[\alpha\beta] - E[\alpha]E[\beta] = C[\alpha, \beta]$. Since α and β are both positive, increasing functions of α , we must have $C[\alpha, \beta] > 0$, implying $V[\hat{p}(\mathbf{y})] > V[\bar{p}(\mathbf{y})]$. Sampling from the posterior reduces the variance of the Monte Carlo estimate of $p(\mathbf{y})$.

Appendix D Mixture Sampling for Monte Carlo Filtering in CFMs

D.1 Main Details

As discussed in Section 4.3, the importance sampling strategy for time t prior-to-posterior updating in the CFM simply extends the existing SGDLM analysis to include the missing \mathbf{y}_{e_0t} vector. The latter is sampled from a mixture of normals arising from conditional SGDLM theory. Important technical details for efficient computation using this strategy are noted here. For clarity, we drop the time subscript t and conditioning information set \mathcal{D}_{t-1} throughout this section.

Given Θ, Λ the SGDLM distribution of $(\mathbf{y}'_c, \mathbf{y}'_e)'$ is $N(\alpha, \Sigma)$ where $\alpha = \mathbf{A}\mu$ with $\mathbf{A} = (\mathbf{I} - \Gamma)^{-1}$, and $\Sigma = \Omega^{-1}$ where $\Omega = (\mathbf{I} - \Gamma')\Lambda(\mathbf{I} - \Gamma)$. Calculation of the vector α requires a matrix inversion, and that of Ω simple matrix products (and recognising that Λ is diagonal). We can avoid some other expensive matrix calculations (in particular, we can avoid inverting Ω directly to find Σ) by exploiting the known structure of Ω . In conformably partitioned forms to define notation, we know that

$$\Gamma = \begin{pmatrix} \Gamma_c & \Gamma_{ce} \\ \Gamma_{ec} & \Gamma_e \end{pmatrix}, \quad \alpha = \begin{pmatrix} \alpha_c \\ \alpha_e \end{pmatrix}, \quad \Sigma = \begin{pmatrix} \Sigma_c & \Sigma_{ce} \\ \Sigma'_{ce} & \Sigma_e \end{pmatrix} \quad \text{and} \quad \Omega = \begin{pmatrix} \Omega_c & \Omega_{ce} \\ \Omega'_{ce} & \Omega_e \end{pmatrix}.$$

Using standard theory, we have the following.

- The margin $p(\mathbf{y}_c | \Theta, \Lambda)$ is $N(\alpha_c, \Sigma_c)$ where $\Sigma_c^{-1} = \Omega_c - \Omega_{ce}\Omega_e^{-1}\Omega'_{ce}$. Define and compute \mathbf{B} as the inverse of the lower triangular Cholesky factor of Ω_e , so that $\Omega_e^{-1} = \mathbf{B}'\mathbf{B}$. Further, define and compute $\mathbf{F} = \Omega_{ce}\mathbf{B}'$. It follows that $\Sigma_c^{-1} = \Omega_c - \mathbf{F}\mathbf{F}'$. This is easily computed, as is its determinant, to provide the terms for direct computation of the log p.d.f. $\ell = \log\{p(\mathbf{y}_c | \Theta, \Lambda)\}$ (up to an irrelevant constant) via $\ell = \log(|\Sigma_c^{-1}|)/2 - (\mathbf{y}_c - \alpha_c)' \Sigma_c^{-1} (\mathbf{y}_c - \alpha_c)/2$.
- The conditional $p(\mathbf{y}_e | \mathbf{y}_c, \Theta, \Lambda)$ is normal with mean vector $\alpha_e - \Omega_e^{-1}\Omega'_{ce}(\mathbf{y}_c - \alpha_c)$ and variance matrix Ω_e^{-1} . The MC strategy samples this distribution, and evaluating its parameters efficiently impacts on overall computational efficiency. With \mathbf{B}, \mathbf{F} as defined and already computed above, it easily follows that a single MC sample from $p(\mathbf{y}_e | \mathbf{y}_c, \Theta, \Lambda)$ is efficiently given by $\mathbf{y}_e = \alpha_e - \mathbf{B}'\{\mathbf{F}'(\mathbf{y}_c - \alpha_c) + \mathbf{z}\}$ where $\mathbf{z} \sim N(\mathbf{0}, \mathbf{I})$.

Now, the normal mixture to be sampled has the form

$$p(\mathbf{y}_{e_0} | \mathbf{y}_c) = \sum_{r=1}^R \pi_r(\mathbf{y}_c) p(\mathbf{y}_{e_0} | \mathbf{y}_c, \Theta^r, \Lambda^r)$$

where each $\pi_r(\mathbf{y}_c) \propto p(\mathbf{y}_c | \Theta^r, \Lambda^r)$. The above general theoretical results apply to each component r of this mixture. First, these define efficient computation of the mixture weights $\pi_r(\mathbf{y}_c)$. Sampling then generates a full set of mixture indices via a multinomial draw on cells $1 : R$ with probabilities $\pi_{1:R}(\mathbf{y}_c)$. Given each sampled component, the conditional normal results above apply to sample \mathbf{y}_{e_0} . Note that these matrix calculations will be made only once on each component r drawn (however many times) in the multinomial sample.

D.2 Additional Theoretical Aspects

This strategy assumes that the MC mixture form of the p.d.f. for $\mathbf{y}_{e0t}|\mathbf{y}_{ct}, \mathcal{D}_{t-1}$ in eqn. (3) is in fact the theoretically exact conditional. As noted, a large time $t - 1$ MC sample size R is important in underpinning this.

To clarify this more fundamentally, relabel the mixture of eqn. (3) as $g(\mathbf{y}_{e0t}|\mathbf{y}_{ct}, \mathcal{D}_{t-1})$, explicitly recognizing it as an approximation to the exact conditional $p(\mathbf{y}_{e0t}|\mathbf{y}_{ct}, \mathcal{D}_{t-1})$. The latter is, of course, not available in any useful analytic form, or for direct simulation. The exact joint posterior for the missing data and parameters is easily seen to have the form

$$p(\mathbf{y}_{e0t}, \Theta_t, \Lambda_t|\mathbf{y}_{ct}, \mathcal{D}_{t-1}) \propto p(\mathbf{y}_{e0t}|\mathbf{y}_{ct}, \mathcal{D}_{t-1}) |\mathbf{I} - \Gamma_t|_+ \tilde{p}_t(\Theta_t, \Lambda_t|\mathbf{y}_{ct}, \mathbf{y}_{e0t}, \mathcal{D}_{t-1}).$$

Use of the MC mixture as a component of the importance sampling proposal implies the joint proposal p.d.f. of the form

$$g(\mathbf{y}_{e0t}, \Theta_t, \Lambda_t|\mathbf{y}_{ct}, \mathcal{D}_{t-1}) \propto g(\mathbf{y}_{e0t}|\mathbf{y}_{ct}, \mathcal{D}_{t-1}) \tilde{p}_t(\Theta_t, \Lambda_t|\mathbf{y}_{ct}, \mathbf{y}_{e0t}, \mathcal{D}_{t-1}).$$

The implied importance weight is then simply proportional to

$$|\mathbf{I} - \Gamma_t|_+ \frac{p(\mathbf{y}_{e0t}|\mathbf{y}_{ct}, \mathcal{D}_{t-1})}{g(\mathbf{y}_{e0t}|\mathbf{y}_{ct}, \mathcal{D}_{t-1})}.$$

This makes transparent the fact that assuming the MC mixture form for the marginal posterior for the missing data leads to the usual SGDLM IS weight based on the determinantal term. It also clearly shows: (i) how intractable a direct IS approach is, since the target marginal $p(\mathbf{y}_{e0t}|\mathbf{y}_{ct}, \mathcal{D}_{t-1})$ cannot be evaluated; and (ii) that even if it could be, the computational burden would escalate due to the need to evaluate the mixture p.d.f. in the denominator of the weight.

Appendix E GDP Case Study

E.1 Parental Sets and Graphs

The chosen set of parental predictors is based on a simple exploratory analysis of the pre-1990 data. This looked at simple regression of the outcomes for each country on all other simultaneous outcomes, with simple forward/backward least squares regression selection of each series on all of the others define a sparse set of parental sets $sp(j)$. The series order is irrelevant to analysis, but graphical summaries here chosen for visual presentations are based the adjusted version of R^2 per series given by the general variable prioritization metric of Crawford et al. (2019). The order was then modified to align with the common parental sets and the resulting factor structure.

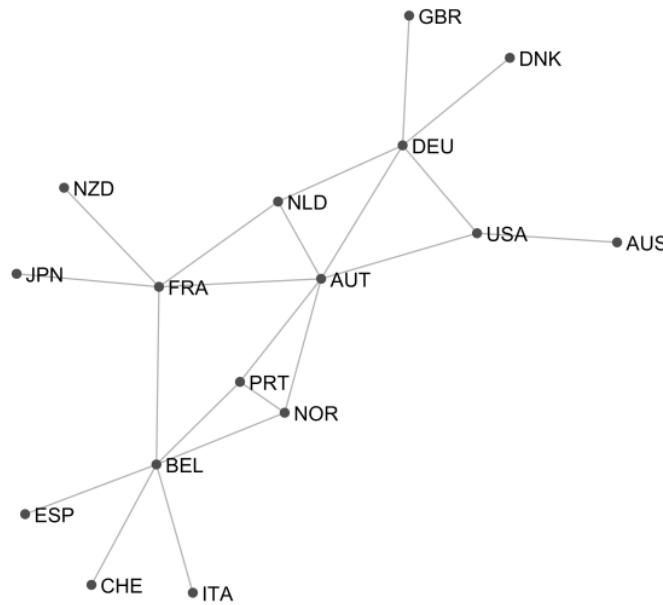


Figure 10: GDP example: Conditional independence graph with the 16 countries as nodes.

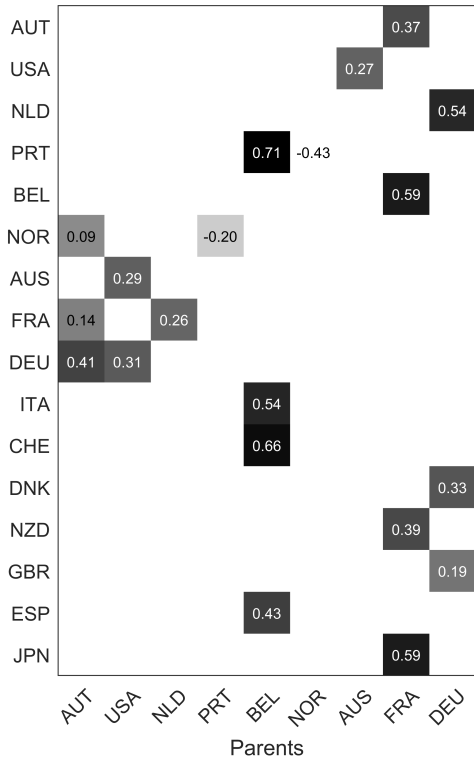
With this parental graph, Γ_t has 7 zero columns corresponding to series that are not parental predictors of any other, and $\text{rank}(\Gamma) = 9$. There are 5 common parental sets; in (arbitrary) order chosen for presentation only, these are (a) $\mathcal{P}_1 = \{\text{DEU}\}$, (b) $\mathcal{P}_2 = \{\text{FRA}\}$, (c) $\mathcal{P}_3 = \{\text{AUS}\}$, (d) $\mathcal{P}_4 = \{\text{BEL}, \text{NOR}\}$ and (e) $\mathcal{P}_5 = \{\text{AUT}, \text{USA}, \text{NLD}, \text{PRT}\}$. The conditional independence graph in Figure 10 shows the map from simultaneous regressions to the implied complete conditional regressions. For 8 countries, e.g., GBR and JPN, the simultaneous and complete conditional distributions are the same; 7 of this set of 8 countries are not simultaneous parental predictors at all, while AUS is both parent and child of USA with no other simultaneous links. The complete conditionals of the other 8 countries differ from the simultaneous conditionals, e.g. DEU is predicted by (AUT, USA) in the simultaneous model, but has the richer set of predictors (AUT, USA, NLD, DNK, GBR) in its complete conditional.

As a side note, the directed simultaneous parental graph in Figure 2 evidently has cycles. Figure 10 displays the implied (conditional independence) graph defining the sparsity pattern in Ω . As a further aside of theoretical interest in the broader graphical modelling area (e.g. Jones et al., 2005; Jones and West, 2005) this graph is non-decomposable.

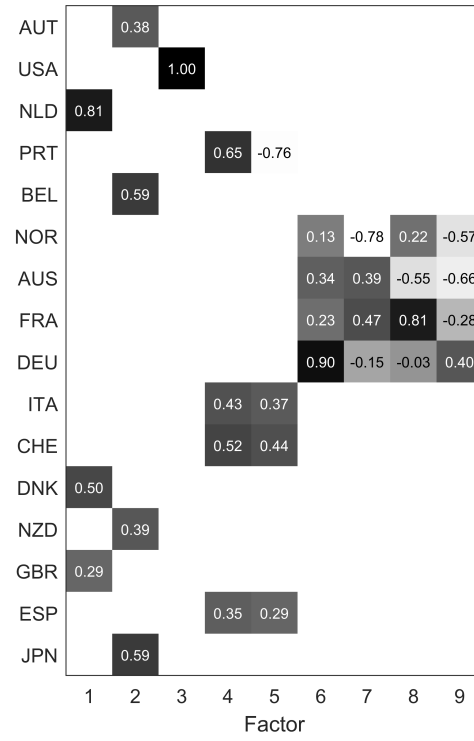
E.2 Aspects of GDP Factor Structure

To compare with the summaries of inferences on aspects of dynamic factor structure in Section 5.6, Figures 11 and Figures 12 are from years $t = 1991$ and 1993. These highlight the time-variation in elements of the regression matrix and then the implied estimated factor loadings and scores. Note, in particular, relatively smooth changes over 1989–1990 and then more marked differences in 1993. The latter relates to the impact of the reunification intervention but overlaid and confounded by the developing recession over those years across the Western economies, in particular, related to a range of additional, potentially causal contributors.

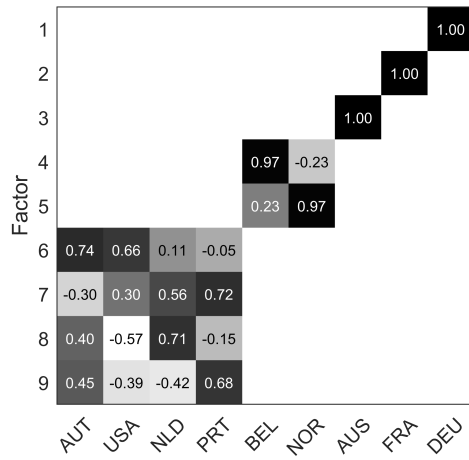
As discussed in Section 5.6, inference on factor structure based on the on-line, filtered posterior Monte Carlo samples is accessible for full uncertainty characterisation. Figures 13 and 14 give examples, showing trajectories of the 4 selected factors. These closely correspond to the plug-in point estimates of Figure 9 of the paper, while adding relevant uncertainty measures.



(a) Regression matrix $\Gamma_t: t = 1990$

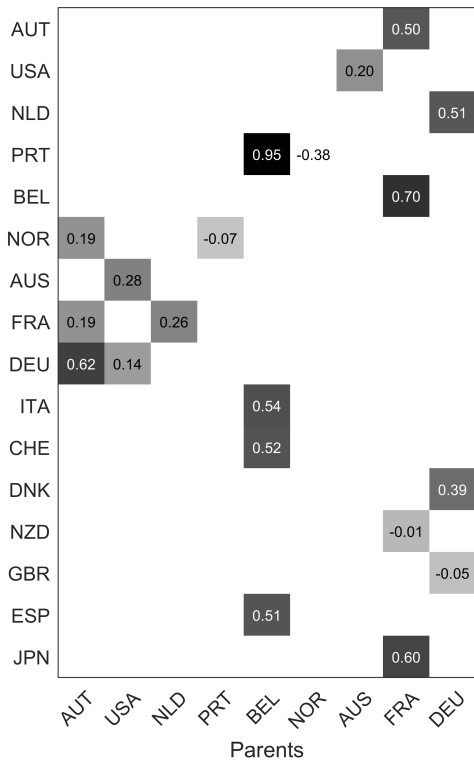


(b) Loadings matrix $L_t: t = 1990$

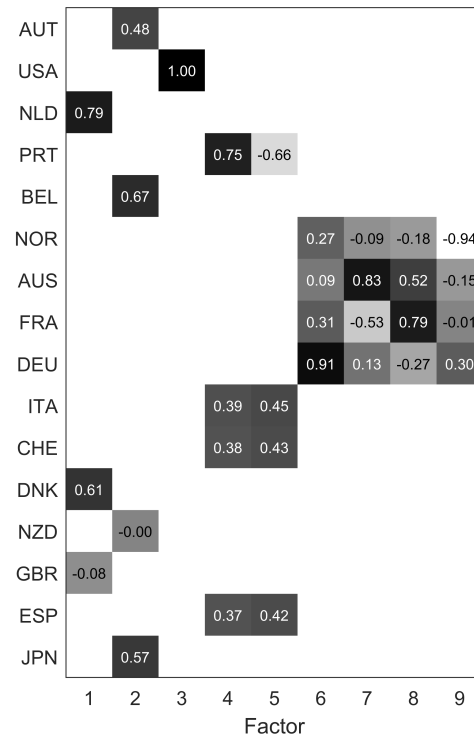


(c) Scores matrix $S_t: t = 1990$

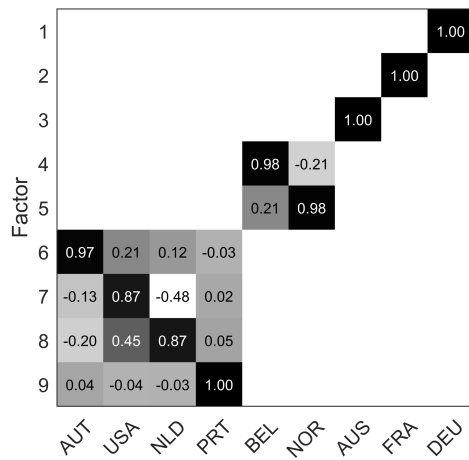
Figure 11: GDP example: Sparsity patterns of model and factor structure at $t = 1990$, with details and format as in the $t = 1989$ example of Figure 8.



(a) Regression matrix $\Gamma_t: t = 1993$



(b) Loadings matrix $L_t: t = 1993$



(c) Scores matrix $S_t: t = 1993$

Figure 12: GDP example: Sparsity patterns of model and factor structure at $t = 1993$, with details and format as in the $t = 1989$ example of Figure 8.

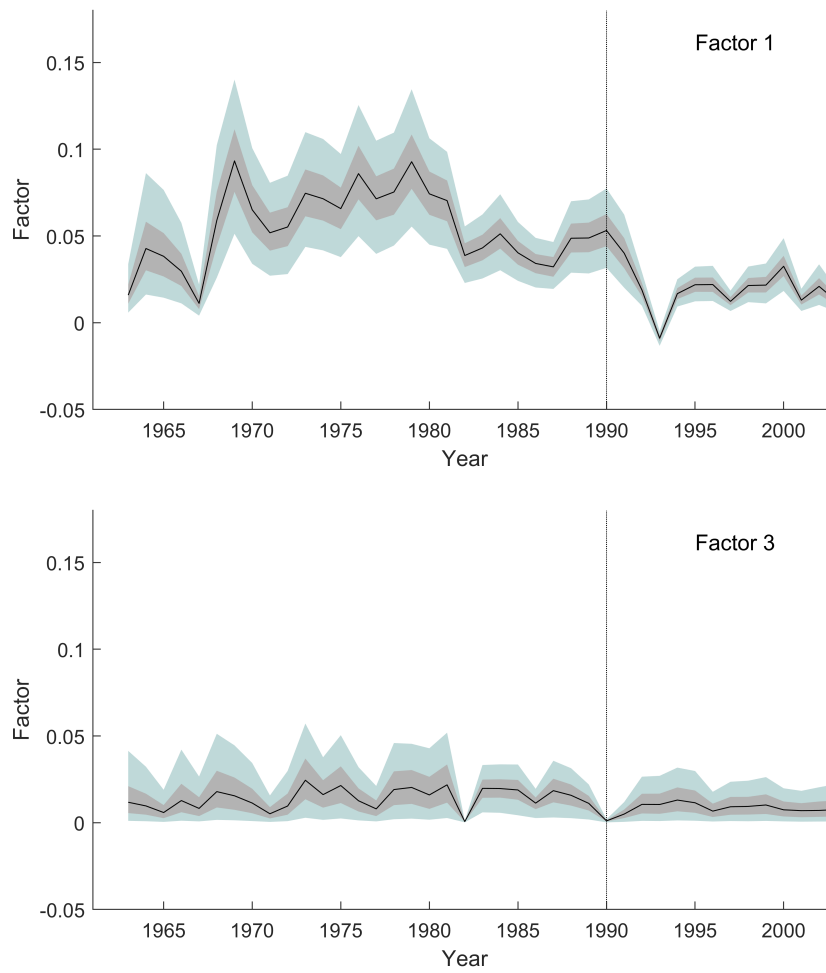


Figure 13: GDP example: Full trajectories of factors 1 and 3 from the filtered Monte Carlo posteriors: 90% intervals (light shading), 50% intervals (darker shading) and medians (full line).

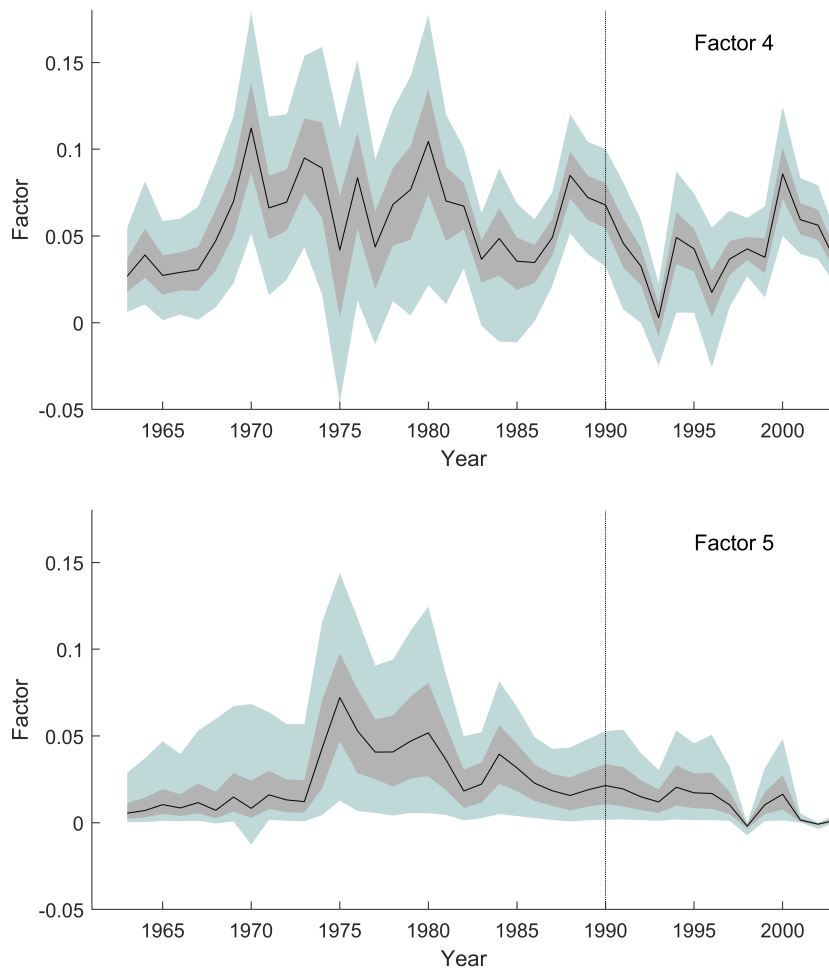


Figure 14: GDP example: Full trajectories of factors 4 and 5 from the filtered Monte Carlo posteriors: 90% intervals (light shading), 50% intervals (darker shading) and medians (full line).

E.3 SGDLM Discount Factor Selection

The discount factors $\beta = 0.95$ and $\delta = 0.95$ were chosen from among all 16 combinations of $\delta, \beta \in \{0.9, 0.95, 0.98, 1\}$. SGDLMs run up to $t = 1990$ generate cumulative log marginal likelihoods displayed in Figure 15; these are shown relative to a baseline of the best-performing model with $\delta = \beta = 0.95$ over the time period. The state evolution discount factor δ is more important to one-step ahead predictive accuracy than the volatility evolution discount factor β , evident from the graph. Beginning in the early 1970s, models with $\delta = 0.95$ and $\delta = 0.98$ begin to outperform models with more adaptive state parameters and more stable volatilities. In the early 1980s, the less adaptive models with $\delta = 0.98, 1$ have brief resurgence, but the model with $\beta = 0.95$ and $\delta = 0.95$ has highest marginal likelihood by the end of the pre-intervention period.

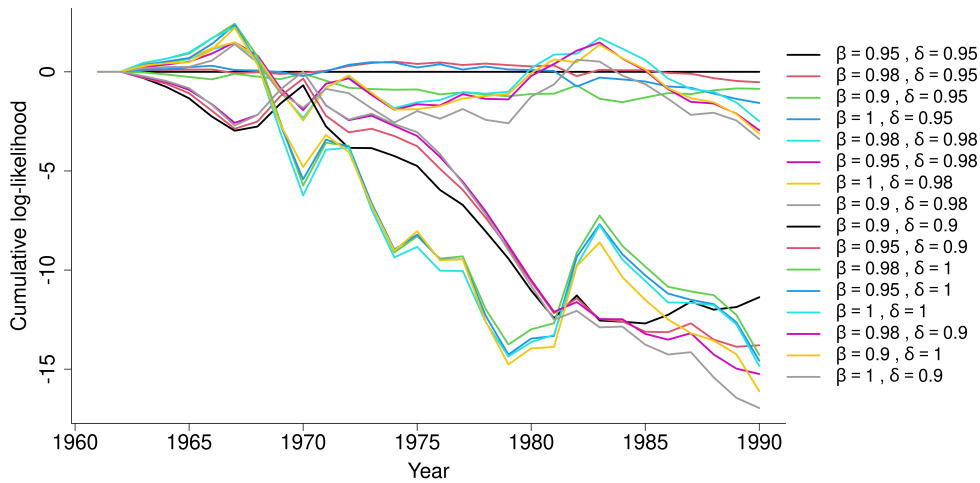


Figure 15: Cumulative log-likelihood comparisons for discount factors.